Title

EFFECT OF A STRAIN INDUCED TRANSFORMATION ON THE TOUGHNESS OF HIGH STRENGTH MATERIALS.

Author

Laporte, Christian Pierre.

Publication Date

1967-09-01

Thesis/dissertation

UCRL-17810

c.2

University of California

Ernest O. Lawrence Radiation Laboratory

EFFECT OF A STRAIN INDUCED TRANSFORMATION ON THE TOUGHNESS OF HIGH STRENGTH MATERIALS

Christian Pierre Laporte
(M. S. Thesis)

September 1967

Berkeley, California

DISCLAIMER

UCRL-17810

UNIVERSITY OF CALIFORNIA
Lawrence Radiation Laboratory
Berkeley, California

AEC Contract No. W-7405-eng-48

EFFECT OF A STRAIN INDUCED TRANSFORMATION ON THE TOUGHNESS OF HIGH STRENGTH MATERIALS

Christian Pierre Laporte

(M.S. Thesis)

September 1967

Table of Contents

EFFECT OF A STRAIN INDUCED TRANSFORMATION ON THE TOUGHNESS OF HIGH STRENGTH MATERIALS

Christian Pierre Laporte

Inorganic Materials Research Division, Lawrence Radiation Laboratory,
Department of Mineral Technology, College of Engineering,
University of California, Berkeley, California

September 1967

ABSTRACT

This investigation was concerned with the fracture toughness of steels which usually exhibit a good combination of strength and ductility. The principal variables investigated by fracture testing single-edge-notched specimens were the amount of carbon in the steels and the temperature of previous deformation.

The toughness was found most sensitive to rolling temperature at low testing temperatures, but seemed to keep a constant value in the vicinity of M_D.

Rolling performed at 450°C depressed the temperature M_D and, thus, the amount of martensite induced during straining. For this temperature the toughness has been found very low, especially for the lowest carbon-content alloy.

Good values of toughness (100 - 130 ksi $\sqrt{in}$) found for alloys whose strength was varying from 130 ksi to 200 ksi should still accompany higher strength levels (250 ksi) with a steady ductility (25%).

I. INTRODUCTION

Early attempts to use high-strength materials in pressure vessels and other structures indicates that mechanical-property specifications based on the usual strength and ductility criteria were not sufficient to assure satisfactory performance. It is the purpose of this investigation to determine the fracture characteristics of materials which exhibit unusually good combinations of strength and ductility.

In spite of their low strength, austenitic alloys are used extensively because of their high ductility, their high corrosion resistance and their lack of ductile to brittle fracture transition. Many attempts have been made to increase their strength. They can be strengthened by cold working.[1] But when the steels are stable against strain-induced-transformation to martensite, the strengthening by cold-work is small (i.e., the strength is less than 125 ksi). When the martensitic transformation occurs during rolling, the strengthening is high but the ductility is lost. Another way of strengthening is to induce precipitation on structural defects in the austenitic matrix. Honeycombe et al.,[2] who investigated this process, obtained yield strengths of 60 ksi. for stainless steels.

In the present study a high alloy austenite was stabilized against transformation by a thermomechanical treatment which simultaneously produced the strengthening precipitate. It has been suggested that precipitates produced during thermomechanical treatment may be more effective than those produced by heat treatment alone.[3] In this way it was possible to obtain an austenite hardened by precipitates and cold work. The purpose of this work was, then, to determine whether or not high fracture thoughness accompanied the excellent combinations of strength and ductility achieved in these materials.

II. MATERIALS PREPARATION

The steels which were used for this study were prepared by induction melting of high purity elements in an helium atmosphere. Their respective compositions are shown in Table 1. The ingots, after being annealed, were forged at 2000°F to a thickness of 1/2 inch. This material was then hot rolled at 900°C - 1000°C to a thickness of 0.250 inch. At room temperature the samples were mostly austenitic. Cold rolling was then performed at room temperature, 250°C, 350°C, 450°C, 550°C reducing the thickness of the samples to 0.050 inch. Some of the material rolled at room temperature was tempered at 450°C for one hour.

Single-edge-notched specimens were then prepared. The tests were performed on an Instron Testing machine at various temperatures ranging from -200°C to +200°C in various baths. The plastic zone and macrostructure of the tested specimens were examined by optical microscopy. The transformation of austenite into martensite was qualitatively checked with a simple magnet. Alloy I, whose carbon content was higher, received a similar treatment but was deformed 20%, 40%, 60% and 80% at 450°C and tested only at room temperature.

A very interesting way of delineating the plastic zone in which transformation has taken place was to spray fluorescent magnetized particles (Magnaflux) on a specimen which had previously been placed in a magnetic field. Since the materials studied here were very resistant to corrosion and etchants, this technique was very useful for observation of the transformed area through the thickness.

III. EXPERIMENTAL PROCEDURES

The single-edge-notched specimen proposed by Sullivan[4] has been used for determination of the fracture toughness. Its shape and size are fully described in Fig. 1. With a standard notch length of $\frac{W}{3}$ the normalized equation:

$$EG = K^2(1 - \nu^2) = \alpha \sigma^2 W \qquad (1)$$

is used for calculation. E is the Young's modulus, G the strain energy release rate,[5] K the fracture toughness, σ is the gross stress (or load divided by unnotched area) and W the width of the specimen. The numerical quantity α has been established by the compliance method pending a theoretical stress analysis for this specimen.[4] The stress used in Eq. (1) is the value reached at the onset of slow (stable) crack growth. When the state of stresses throughout the loading has been predominant by plane strain, the fracture toughness is noted K_{ic}. In plane stress conditions, the toughness is noted, K_c.[5] In any case the value of K has been calculated according to the compliance curve given by Sullivan[4] and reproduced on Fig. 1. In the case of a single-edge notch of length $a_o = \frac{W}{3}$ which was currently used for this work, K is determined by:

$$K^2 = 9.5 \frac{\sigma^2 W}{1-\nu^2} \qquad (2)$$

To determine whether fracture occurs in plane strain or in plane stress conditions, was a difficult issue since the specimens were very small and the sensitivity of the Instron machine was not sufficient to detect the onset of slow crack growth. Then, for certain cases, thicker specimens were prepared to determine whether or not the fracture mode was dependent on the specimen thickness.

All the attempts to solve this problem are fully described in the appendix. A definite answer having not been reached for reasons explained further, the label K was used for the toughness computed from Eq. (2). The stress σ was calculated from the maximum load at fracture.

IV. RESULTS AND DISCUSSION

The values of K, computed from the maximum load at fracture, are shown for alloys A, B, C and D in Tables 2 to 7. Each table is related to a particular mode of cold work and includes the tests performed in liquid nitrogen (-196°C), dry ice (-76°C), ambient atmosphere (+20°C), boiling water (+100°C), and heated oil at 200°C. Tensile properties (yield strength, σ_{ys}, elongation, ultimate tensile strength: u.t.s.) determined under the same conditions are also shown, and the characteristics of the fracture mode (i.e., plastic zone size, shape of crack, speed of propagation, mode of fracture) are also indicated. The magnetic response of each specimen, measured as described in the experimental procedures and performed before and after the fracture is reported in the tables. It is thus noticed that all alloys are strongly martensitic when they are rolled at room temperature. But alloy A is the only martensitic material after cold work if rolling has been performed above 250°C. The magnet technique always detected an increase in the amount of martensite along and at the tip of the crack except when the tests were run at 200°C. At this temperature alloys A and B showed very little transformation and only in a very small zone along the crack. No transformation was detected for alloys C and D at 200°C. This shows that the temperature M_D above which martensite cannot be induced by deformation is slightly above 200°C for alloys A and B and between 100°C and 200°C for alloys C and D. A better approximation of the value of M_D can be reached by testing each alloy at intermediate temperatures between 100°C and 250°C and using the magnet technique before and after testing.

A. Influence of Testing Temperature

The effect of the martensitic transformation on fracture toughness can be seen on the plots of toughness versus testing temperatures (Figs. 2 to 4). The variation of K with temperature observed below 100°C is reversed or reduced at 200°C where the induced transformation is no longer a main factor in the fracture process. Some interesting conclusions can be drawn from these figures:

Below M_D, the slopes of the curves for materials rolled at 250°C are negative and decreasing in their absolute value as the carbon content increases. Conversely, for materials rolled at 450°C and 550°C the slopes are positives and keep an approximately constant value for different carbon contents. As an intermediate situation, the materials rolled at 350°C show a negative slope decreasing in absolute value with increasing carbon (alloy A-C) but a positive slope for alloy D.

It is also remarkable that, at almost all testing temperatures, the best value of K is obtained for all alloys when the rolling is done at 250°C. In the vicinity of M_D the toughness seems to become relatively insensitive to testing temperatures compared to the behaviour at lower temperatures.

Although no strain induced transformation can occur above M_D, experiments above 200°C should be conducted in order to ascertain the constancy of K.

B. Influence of Rolling Temperature

The importance of the rolling temperature on the toughness is clearly shown on Figs. 6-10. Alloys A and C are very similar in their behaviour. As previously shown the toughness reaches a maximum for rolling at 250°C, then decreases to a minimum value at 450°C before increasing again at 550°C. Alloys B and D seem less sensitive to rolling temperature than alloys A and C except for tests conducted at liquid nitrogen temperatures. There is no longer a drastic change of behaviour at 450°C. However, for any of the four alloys the variations of toughness with rolling temperature became more accentuated as the testing temperature was decreased. The magnet technique did not allow a quantitative measure of the amount of martensite formed during the test. However, it was observed that the amount of transformation was even less for the specimens cold rolled at 450°C than for those rolled at 250°C, 350°C and 550°C. This is confirmed by the very low values of the elongation and by the magnetic tests conducted on tensile specimens[6] at testing temperatures of 200°C. These results show that M_D is the lowest for specimens rolled at 450°C. This suggests that the transformation could slightly be impeded at any testing temperature when the materials have been rolled at 450°C and could explain the low values of K for this rolling condition.

The different behaviour between alloys A and C on one hand, and B and D on the other hand might be explained by the different contents in alloying elements. Table 1 shows that alloy B has a low molybdenum content and alloy D a low silicon content. Both elements increase the chemical stability of austenite through their effect on M_S and M_D. The formation of alloyed carbides during the processing treatments is probably very important with respect to subsequent martensitic transformation

during testing. Better magnetic measurements would be necessary to ascertain the correlation between toughness and the amount of martensite formed.

C. Strength and Toughness

High fracture toughness is only useful in materials if it is accompanied with good tensile properties. The ductility remains fairly constant for all treatments except in the vicinity of M_D where transformation does not occur. The variations of K/σ_{ys} with σ_{ys} are shown for each alloy in Figs. 10-13. Due to the low values of toughness obtained by rolling at 450°C, the band delineating the results is wider for alloy A (lines a and b in Fig. 10) than for alloys B, C, and D. Setting the bands delineating the results for each specimen on one single Fig. 15, shows that all the points representing all the experiments conducted on the four alloys are inside the area bordered by lines (a) and (a')of alloy A. The slopes of these lines are very important because one is as much interested in keeping high values of K for high values of σ (above 200 ksi) as getting them for lower values of σ. Thus, if one follows the comparison between the four alloys on Fig. 16, one will notice that line (a) represents the most favorable case since it shows the highest values of K/σ_{ys} and the smallest slope in absolute value. For an identical reason line (a') represents the least favorable case below yield strength of 200 ksi, whereas line (b') which is the lower limit for alloy B, will represent the least favorable case above yield strengths of 200 ksi. This assumes that the same pattern of variations of K/σ with σ_{ys} will be repeated above 200 ksi as it was between 130 and 200 ksi. Experiments conducted on alloy J seems to confirm the right to extrapolate. This alloy, which contains more carbon (0.3%) than the previous one, was deformed 25%, 40%, 50% and 80% at 450°C and tested only at room temperature. The results reported on Table 8 provide a range of yield strength from 120 ksi to 220 ksi.

The variations of K and K/σ with σ_{ys} are drawn on Fig. 15. Line (i) from this figure fits perfectly in level and slope with the previous lines on Fig. 15 and extends the results to a yield strength of 220 ksi in a way which was expected by extrapolation. Figure 14 shows that the toughness keeps a fairly constant value when the yield strength varies from 150 ksi to 220 ksi. Extrapolation between 200 ksi and 300 ksi has been done in Fig. 17 in order to compare with conventional and maraging high strength steels.[7] It is remarkable that the slope of the band representing the TRIP alloys is much smaller than the slopes for the other two classes of steels. It must be added that Fig. 17 represents the variations of K_c/σ_{ys} and recalled (see appendix) that the K_{ic} and K_c values might be very close to each other in the case of TRIP steels. All these considerations suggest that high toughness combined with high strength (above 250 ksi) can be obtained in TRIP steels.

V. SUMMARY AND CONCLUSIONS

The objective of this study was to investigate the fracture toughness of high strength stable austenitic steels. The composition of these steels and their preparation which had been previously investigated in this laboratory, were aimed to depress the temperature M_s well below room temperature and to get a high ductility at the same time. The principal variables investigated were the composition of the alloys, and the temperature of deformation. Due to the difficulty of providing alloys with the same exact amounts of alloying elements, the different variables were not satisfactorily separated and a systematic study of the effect of each variable could be performed. Nevertheless some valuable information on the behaviour of TRIP steels against notched-fracture was withdrawn from a large number of tests.

The toughness K was found very sensitive to low testing temperature for low carbon content alloys. In the vicinity of M_D (about 200°C), K remained rather constant (between 110 and 130 ksi $\sqrt{in}$). The variations of K with the temperature of previous deformation were smoother except at 450°C for certain alloys. At this temperature the amount of martensite induced during straining seems unusually low. More sensitive magnetic measurements might show that, in fact, a good value of toughness is obtained with a large amount of martensite induced.

The comparison of the ratio toughness/strength with other high strength alloys allowed the author to foresee for TRIP steels a very good combination of strength (250 ksi) toughness (130 ksi$\sqrt{in}$) and elongation (25%). This will be obtained if a deeper investigation is performed on the influence of each variable on the induced transformation and, thus, on the toughness. More sensitive techniques than the ones used for this work are suggested.

APPENDIX

The question of labeling the fracture toughness K by comparison with the modes of fracture observed in other materials arose during the experiments discussed in this work. When the state of stress throughout the loading is predominantly plane strain the toughness is denotes as K_{ic}. When the state of stress is plane stress, K is denoted as K_c. In order to reach a decision concerning the TRIP alloys, many ways of investigation have been used.

According to Boyle,[8] the step in the loading curve (or crack "pop-in") is representative of plane-strain fracture. This discontinuity has been observed several times on the TRIP alloys as it is shown in Fig. 17 for alloy K. It should be noted, then, that every time a "pop-in" occurred, the "K_{ic}" value computed from the corresponding stress did not differ more than 5% from the plane stress value K_c computed from the maximum stress at fracture. This seems to indicate that K_c and K_{ic} are very close in value. At this time it is not clear why it should be so. The "pop-in" phenomenon, however, did not appear on all loading curves and it could not be decided if this was due to the lack of sensitivity of the Instron or to the lack of plane strain conditions at the onset of crack propagation.(Fig. 18).

Another way of investigating the fracture mode was to cut sections in the specimens and observe the plastic zone through the thickness. This technique was performed on alloys H and I for specimens with a thickness of t = 0.150 inch. Whereas the plastic zone through the thickness in alloy I was of constant size and shape, the one in alloy H showed a reduction in size and a change in shape toward the center (Fig. 19-24). The behavior of alloy I was, thus, more representive of plane strain conditions, whereas the transformed bands appearing in the

center of the thickness of alloy H represented sections of shear planes of plane stress condition of fracture.

Even though the technique of thinning was the safest way to determine the stress state, it was not the quickest and could not possibly be applied on all specimens.

Thicker specimens of alloy I and H were prepared and tested. The results are shown with their pictures on Figs. 25 and 26. Although the size of the plastic zone and the shape of the fracture in alloy I are of a plane stress type for small thicknesses, a trend toward smaller plastic zones and flatter cracks was observed when the thickness was increased. At the same time the value of K was not drastically decreased. This can account for the nearly equal values of K_c and K_{ic}. However, no "pop-in" was observed, even for 0.250" thick specimens.

The best method for determining the plane strain value in order to compare it with the values found in this work, would be to test very thick specimens (1 inch to 2 inches).

Another improvement would be to adapt, at the opening of the notch, a strain gauge which would be more sensitive to detect the "pop-in" than the load cell.

ACKNOWLEDGMENTS

The author is deeply grateful to Professor E. R. Parker, Professor V. F. Zackay and Dr. Dan Merz for their guidance, encouragements, and support throughout the course of this investigation.

This work was performed under the auspices of the United States Atomic Energy Commission through the Inorganic Materials Research Division of the Lawrence Radiation Laboratory, University of California, Berkeley, California.

REFERENCES

1. G. Thomas, D. Schmatz, and W. W. Gerberich, High Strength Materials, V. F. Zackay, Ed., (John Wiley and Sons, Inc., New York, 1965) p. 251.

2. R. W. K. Honeycombe, M. J. Harding, T. J. Irani, High Strength Materials, V. F. Zackay, Ed., (John Wiley and Sons, Inc., New York, 1965), p. 213.

3. A. McEvily, R. Busch, F. Schaller and D. Schwartz, Trans. ASM 56, 753 (1963).

4. R. W. Boyle, A. M. Sullivan, and T. M. Krafft, Determination of Plane Strain Fracture Toughness with Sharply Notched Sheets, Welding Journal Res. Supplement 27, 428 (Sept. 1962).

5. G. T. Hahn, and A. R. Rosenfield, Sources of Fracture Toughness- The Relations between K_{ic} and the Ordinary Tensile Properties of Metals, presented at ASTM Symposium, April 18, 1967.

6. G. Chanani, M. S. Thesis (Sept. 1967) University of California, UCRL-

7. V. F. Zackay, W. W. Gerberich, R. Busch and E. R. Parker, The Strength and Toughness of Dynamically Strain Aged Alloy Steel Sheets, International J. of Fracture Mechanics, 2, (4) 638 (1966).

8. R. W. Boyle, A Method for Determining Crack Growth in Notched Steel Specimens, Materials Research and Standards 2 (8), 646-651 (August 1962).

Table 1. Composition of the alloys used in this work.

		Cr	Ni	Mo	S_l	M_n	C
6698-1	A	12.23	7.69	4.1	1.6	0.68	0.047
6698-2	B	11.64	7.69	2.5	1.3	0.60	0.074
6698-3	C	11.84	7.71	3.0	1.5	0.61	0.155
6698-4	D	11.99	7.71	3.2	0.7	0.52	0.198
674-9	E	8.8	7.48	3.92	1.87	1.37	0.33
674-10	F	8.81	7.48	3.93	1.81	1.40	0.42
674-11	G	8.79	7.51	3.95	1.91	1.40	0.51
675-13	H	12.23	7.69	4.1	1.6	0.68	0.092
675-14	I	11.84	7.71	3.0	1.5	0.61	0.195
676-4	K	10.2	7.9	5.95	3.7	1.3	0.28

Table 2. Summary of test results - 80% Deformation at room temperature.

Testing Temp.	Alloy	K psi$\sqrt{in}$	(1) σ_{ys} ksi	(1) Elongation %	(1) U.T.S. ksi	(2) Magnetic Properties		(3) Plastic zone size mm	(4) Shape of Crack	(5) Speed of Propagation	(6) Mode of Fracture
						Before Test	After Test				
-196°C	A	109	320	2.78	320	M	M	0	s	f	F
	B	125	362	2.40	362	M	M	0	s	f	F
	C	106	386	1.3	382	M	M	0	s	f	F
-76°C	A	130	258	2.8	258	M	M	.5	c	f	S.L.
	B	93	312	1.85	312	M	M	0	s	f	F
	C	108	318	1.85	318	M	M	0	s	f	F
+20°C	A	118	225	2.4	225	M	M	0	c	f	S
	B	97	266	0.56	266	M	M	0	c	f	S
	C	80	290	1.48	290	M	M	0	c	f	F
+100°C	A	112	231	1.85	231	M	M	0	c	f	S
	B	80	269	1.1	269	M	M	0	c	f	S
	C	73	294	1.67	294	M	M	0	c	f	S
+200°C	A	103	223	0.56	223	M	M	0	c	f	S
	B	70	259	1.1	259	M	M	0	c	f	S
	C	81	282	1.7	282	M	M	0	c	f	S

1) Results given by G. Chanani (Master Thesis).
2) A For austenitic state; M for martensitic state; M' very small amount of martensite.
3) Average dimension of plastic zone on each size of crack given in mm.
4) s for streight; c for curved.
5) f for fast; s for slow.
6) F for 100% flat; S for 100% shear; S.L. for shear lips.

Table 3. Summary of test results - 80% Deformation at room temperature and tempered at 450°C.

Testing Temp.	Alloy	K psi$\sqrt{in}$	σ_{ys} (1) ksi	Elongation (1) %	U.T.S. (1) ksi	Magnetic Properties (2) Before Test	Magnetic Properties (2) After Test	Plastic zone size mm (3)	Shape of Crack (4)	Speed of Propagation (5)	Mode of Fracture (6)
-196°C	A	106	386	1.66	386	M	M	0	s	f	F
	B	106	407	0.18	407	M	M	0	s	f	F
	C	85	425	0.41	425	M	M	0	s	f	F
-76°C	A	116	322	2	322	M	M	0	s	f	S.L.
	B	91	355	1.3	355	M	M	0	s	f	F
	C	86	367	1.5	367	M	M	0	s	f	F
+20°C	A	136	298	2	298	M	M	0	s	f	S
	B	94	331	0.37	331	M	M	0	s	f	F
	C	101	337	0.37	337	M	M	0	s	f	S.L.

1) Results given by G. Chanani (Master Thesis).

2) A for austenitic state; M for martensitic state; M' very small amount of martensite.

3) Average dimension of plastic zone on each size of crack given in mm.

4) s for straight; c for curved.

5) f for fast; s for slow.

6) F for 100% flat; S for 100% shear; S.L. shear lips.

Table 4. Summary of test results -- 80% Deformation at 250°C.

Testing Temp.	Alloy	K psi$\sqrt{in}$	σ_{ys} ksi (1)	Elongation % (1)	U.T.S. ksi (1)	Magnetic Properties (2) Before Test	Magnetic Properties (2) After Test	Plastic zone size mm (3)	Shape of Crack (4)	Speed of Propagation (5)	Mode of Fracture (6)
-196°C	A	157	193	21.8	315	M'	M	1	s	f	S
	B	140	186	17.8	322	A	M	.3	s	f	F
	C	140	191	18.3	330	A	M	.5	s	f	F
	D	123	209	18.7	346	A	M	.4	s	f	F
-76°C	A	140	136	15.5	235	M'	M	2.5	c	s	S
	B	125	142	18.8	250	A	M	2.5	c	s	S
	C	132	163	20	261	A	M	2	s	f	F
	D	120	170	20.7	267	A	M	1	s	f	F
+20°C	A	127	138	16.8	192	M'	M	2.5	c	s	S
	B	118	148	18.8	205	A	M	2.5	c	s	S
	C	136	161	21.8	214	A	M	2	s	s	S
	D	116	190	26.3	226	A	M	0.7	s	f	F
+100°C	A	116	168	22.4	169	M'	M	1	s	f	F
	B	118	193	22.6	193	A	M	1	s	f	F
	C	109	189	22.7	189	A	M	1	s	f	F
	D	113	208	16.8	208	A	M	.7	s	s	F
+200°C	A	140	174	3.7	174	M'	M	1	s	f	S
	B	125	175	9.8	175	A	M'	1	s	f	S.L.
	C	134	179	5	179	A	A	1	s	f	F
	D	122	186	4.3	186	A	A	1	s	f	F

1) Results given by G. Chanani (Master Thesis).
2) A for austenitic state; M for martensitic state; M' very little amount of martensite.
3) Average dimension of plastic zone on each size of crack given in mm.
4) s for straight; c for curved.
5) f for fast; s for slow.
6) F for 100% flat; S for 100% shear; S.L. Shear Lips.

Table 5. Summary of test results - 80% deformation at 350°C.

Testing Temp.	Alloy	K psi$\sqrt{in}$	σ_{ys} ksi (1)	Elongation % (1)	U.T.S. ksi (1)	Magnetic Properties (2) Before Test	Magnetic Properties (2) After Test	Plastic zone size mm (3)	Shape of Crack (4)	Speed of Propagation (5)	Mode of Fracture (6)
-196°C	A	140	177	20	327	M'	M	1	s	f	S
	B	124	173	22	344	A	M	.5	s	f	F
	C	128	179	19	348	A	M	1	s	f	F
	D	106	188	14	323	A	M	.5	s	f	F
-76°C	A	129	125	17	219	M'	M	3	c	f	S
	B	120	139	17.6	241	A	M	1.5	s	f	F
	C	128	146	20	249	A	M	2	s	f	F
	D	105	145	15	260	A	M	1	s	f	F
+20°C	A	130	128	18	177	M'	M	2	c	s	S
	B	121	144	20	205	A	M	1.5	c	s	S
	C	123	149	19	213	A	M	1.5	s	f	F
	D	116	156	20	215	A	M	1	s	f	F
+100°C	A	113	149	23	152	M'	M	1	s	s	S
	B	121	167	35	175	A	M	1	s	s	F
	C	127	174	34	179	A	M	1	s	s	F
	D	117	182	29	190	A	A	.7	s	f	F
+200°C	A	124	158	3.9	158	M'	M	.7	s	s	F
	B	123	166	5.2	166	A	A	.7	s	s	F
	C	120	174	5	174	A	A	1	s	s	F
	D	122	183	5	183	A	A	1	s	s	F

1) Results given by G. Chanani (Master Thesis).
2) A for austenitic state; M for martensitic state; M' very small amount of martensite.
3) Average dimension of plastic zone on each size of crack given in mm.
4) s for straight; c for curved.
5) f for fast; s for slow.
6) F for 100% flat; S for 100% shear; S.L. shear lips.

Table 6. Summary of test results - 80% deformation at 450°C.

Testing Temp.	Alloy	K psi$\sqrt{in}$	(1) σ_{ys} ksi	(1) Elongation %	(1) U.T.S. ksi	(2) Magnetic Properties		(3) Plastic zone size mm	(4) Shape of Crack	(5) Speed of Propagation	(6) Mode of Fracture
						Before Test	After Test				
-196°C	A	83	187	11.95	235	M'	M	.5	s	s	F
	B	102	167	23.4	322	A	M	.5	s	f	F
	C	96	174	23.7	348	A	M	.5	s	f	F
	D	88	188	24.6	361	A	M	1	s	f	F
-76°C	A	100	155	16.6	215	M'	M	.5	s	f	S.L.
	B	110	141	19.8	235	A	M	1	c	s	S.L.
	C	103	142	20.7	248	A	M	1	s	f	F
	D	97	165	13.3	239	A	M	1	s	f	F
+20°C	A	100	153	22.5	185	M'	M	1.5	s	f	S
	B	110	150	21.46	198	A	M	2	s	s	S
	C	111	152	23.7	209	A	M	2.5	s	s	S
	D	102	161	22.6	218	A	M	1	s	f	F
+100°C	A	110	168	5.3	167	M'	M	.7	s	s	F
	B	117	159	27.8	163	A	M	1.5	s	s	F
	C	114	181	28.3	182	A	M	1	s	s	F
	D	114	176	35.9	181	A	M	1	s	f	F
+200°C	A	98	171	2.7	171	M'	M	0.5	s	f	S.L.
	B	115	162	3.7	162	A	A	1	s	s	S.L.
	C	114	169	2.6	168	A	A	1	s	s	S.L.
	D	109	171	4.4	171	A	A	1	s	s	F

1) Results given by G. Chanani (Master Thesis).
2) A for austenitic state; M for martensitic state; M' for very small amount of martensite.
3) Average dimension of plastic zone on each size of crack given in mm.
4) s for straight; c for curved.
5) f for fast; s for slow.
6) F for 100% flat; S for 100% shear; S.L. shear lips.

Table 7. Summary of test results - 80% deformation at 550°C.

Testing Temp.	Alloy	K psi√in	(1) σ_{ys} ksi	(1) Elongation %	(1) U.T.S. ksi	(2) Magnetic Properties Before Test	(2) Magnetic Properties After Test	(3) Plastic zone size mm	(4) Shape of Crack	(5) Speed of Propagation	(6) Mode of Fracture
-196°C	A	110	170	15.2	265.5	M'	M	1	s	f	F
	B	95	176	15.2	280	A	M	0.5	s	f	F
	C	98	174	22.2	337	A	M	0.5	s	f	F
	D	92	185	13	260	A	M	0.5	s	f	F
-76°C	A	115	149	15.5	225	M'	M	1	s	s	S
	B	105	131	18.3	237	A	M	1	s	f	F
	C	108	140	20.2	253	A	M	1	s	f	F
	D	92	143	19.2	251	A	M	1	s	f	F
+20°C	A	122	161	18.7	191	M'	M	3	c	s	S
	B	104	136	19.8	207	A	M	3	c	s	S
	C	121	142	19.2	215	A	M	1.5	s	s	S.L.
	D	101	128	22.6	225	A	M	1	s	f	F
+100°C	A	119	158	10.7	157	M'	M	2	c	s	S
	B	122	157	26.8	174	A	M	1	s	s	S.L.
	C	128	150	35.2	176	A	M	1	s	s	F
	D	123	178	30.34	189	A	M	1.5	s	f	F
+200°C	A	114	141	3.15	141	M'	M	0.5	s	f	S.L.
	B	120	147	5.55	147	A	M'	0.5	s	s	F
	C	115	157	4.44	157	A	A	0.5	s	s	F
	D	118	163	4.44	163	A	A	0.5	s	s	F

1) Results given by G. Chanani (Master Thesis).
2) A for austenitic state; M for martensitic state; M' for very small amount of martensite.
3) Average dimension of plastic zone on each size of crack given in mm.
4) s for straight; c for curved.
5) f for fast; s for slow.
6) F for 100% flat; S for 100% shear; S.L. Shear Lips.

Table 8. Tensile and fracture characteristics of alloy K for different thicknesses and amount of deformation.

Amount of Deformation	Thickness	K psi$\sqrt{in}$	(1) σ_{ys} ksi	(1) Elongation %	(1) U.T.S. ksi	(2) Magnetic Properties		(3) Plastic zone size mm	(4) Shape of Crack	(5) Speed of Propagation	(6) Mode of Fracture
						Before Test	After Test				
20%	0.050	119	127	42	163	A	A	1	s	s	S.L.
	0.100	114				A	A	1	s	f	S.L.
	0.150	112				A	A	2	s	f	F
	0.200	120				A	A	2.5	s	f	F
40%	0.050	130	175	36	190	A	A	1	s	s	S.L.
	0.100	120				A	A	1.5	s	f	S.L.
	0.150	124				A	A	2	s	f	F
	0.200	122				A	A	2.5	s	f	S.L.
60%	0.050	115	200	26	200	A	A	.7	s	f	S.L.
	0.100	125				A	A	1	s	f	S.L.
	0.150	124				A	A	1.5	s	f	S.L.
	0.200										
80%	0.050	118	220	20	210	A	A	.5	s	f	S
	0.100										
	0.150										
	0.200										

1) Results given by standard tensile specimen: 1 inch gage length.
2) A for austenitic; M for martensitic.
3) Average size of plastic zone on each size of crack.
4) s for straight; c for curved.
5) f for fast; s for slow.
6) F for 100% flat; S for 100% shear; S.L. Shear Lips.

FIGURE CAPTIONS

Fig. 1 Compliance curve and notched specimen used for determination of K.

Fig. 2 Relation between K and testing temperature for alloy A.

Fig. 3 Relation between K and testing temperature for alloy B.

Fig. 4 Relation between K and testing temperature for alloy C.

Fig. 5 Relation between K and testing temperature for alloy D.

Fig. 6 Relation between K and rolling temperature for alloy A.

Fig. 7 Relation between K and rolling temperature for alloy B.

Fig. 8 Relation between K and rolling temperature for alloy C.

Fig. 9 Relation between K and rolling temperature for alloy D.

Fig. 10 Relation between K/σ_{ys} and σ_{ys} for alloy A.

Fig. 11 Relation between K/σ_{ys} and σ_{ys} for alloy B.

Fig. 12 Relation between K/σ_{ys} and σ_{ys} for alloy C.

Fig. 13 Relation between K/σ_{ys} and σ_{ys} for alloy D.

Fig. 14 Variation of K and K/σ_{ys} versus σ_{ys} for alloy K.

Fig. 15 Variation of K/σ_{ys} versus σ_{ys} for alloys A, B, C, D, K. altogether.

Fig. 16 Situation of the TRIP steels in the plot of K/σ_{ys} versus σ_{ys} compared with conventional and maraging steels.

Fig. 17 Loading curve of alloy K for two thicknesses showing the "pop-in" before fracture. This alloy had previously been deformed 60% at 450°C.

Fig. 18 Loading curves of alloy K for two thicknesses showing the "pop-in" before fracture in the .150" thick specimen. This alloy had been previously deformed 40% at 450°C.

Fig. 19 Drawing showing the section of specimen K in which the plastic zones were examined.

Fig. 20 Picture taken of the crack and the plastic zone in the core of specimen K.

Fig. 21 Plastic zone at the surface of the specimen.

Fig. 22 Plastic zone at t/6 under the surface.

Fig. 23 Plastic zone at t/3 under the surface.

Fig. 24 Plastic zone at t/2 under the surface or at the core of the specimen.

Fig. 25 Picture showing the variations of the shape of the crack in alloy I when the thickness of the specimen is increased.

Fig. 26 Picture showing the variations of the shape of the crack in alloy H when the thickness of the specimen is increased.

Fig. 27 Picture showing the variations of the shape of the crack in alloy K when the thickness of the specimen is increased.

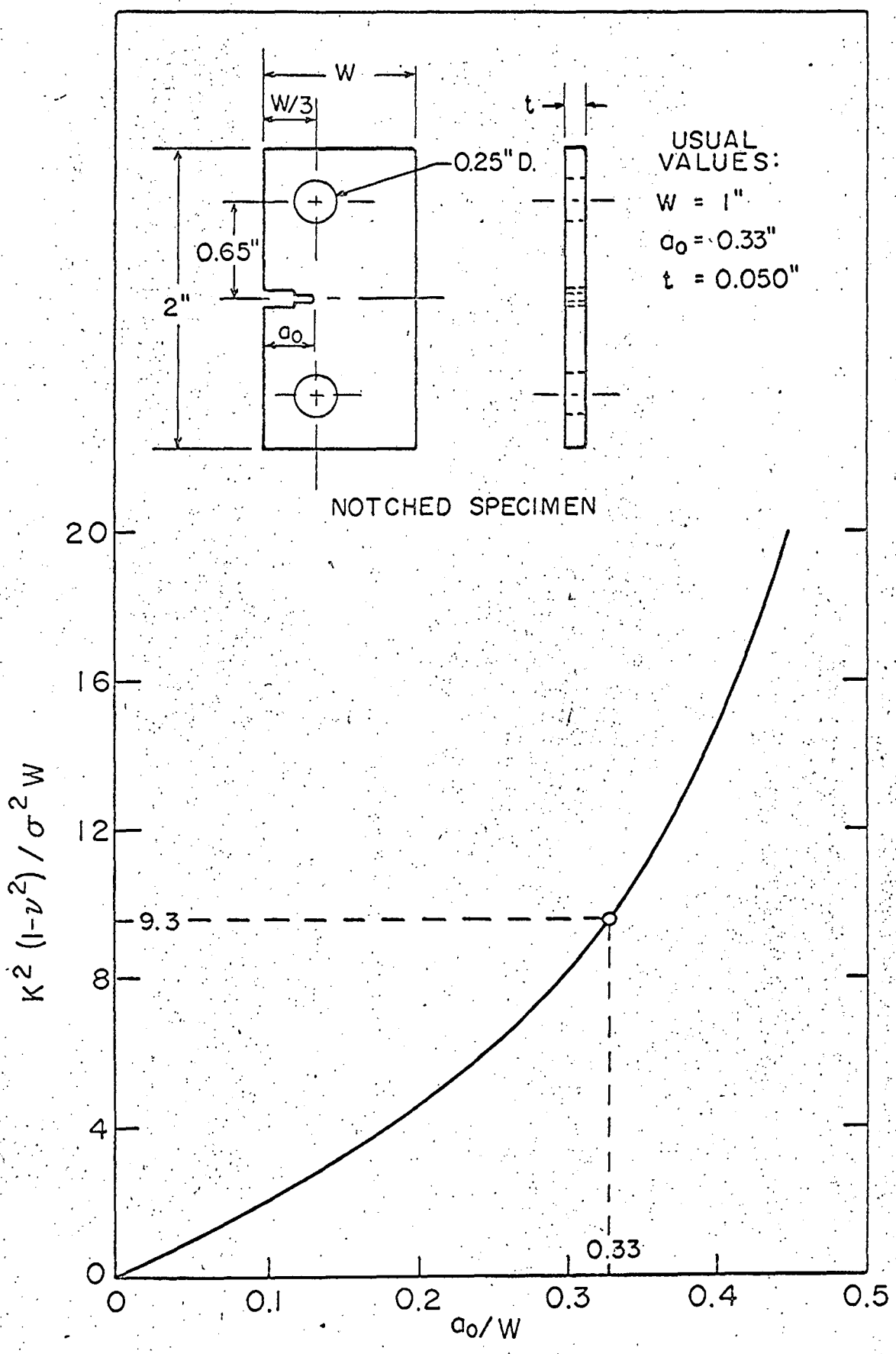
W
W/3
t
0.25" D.
USUAL VALUES:
W = 1"
a_o = 0.33"
t = 0.050"
0.65"
2"
a_o
NOTCHED SPECIMEN
$K^2(1-\nu^2)/\sigma^2 W$
20
16
12
9.3
8
4
0
0
0.1
0.2
0.3
0.33
0.4
0.5
a_o/W

Fig. 1

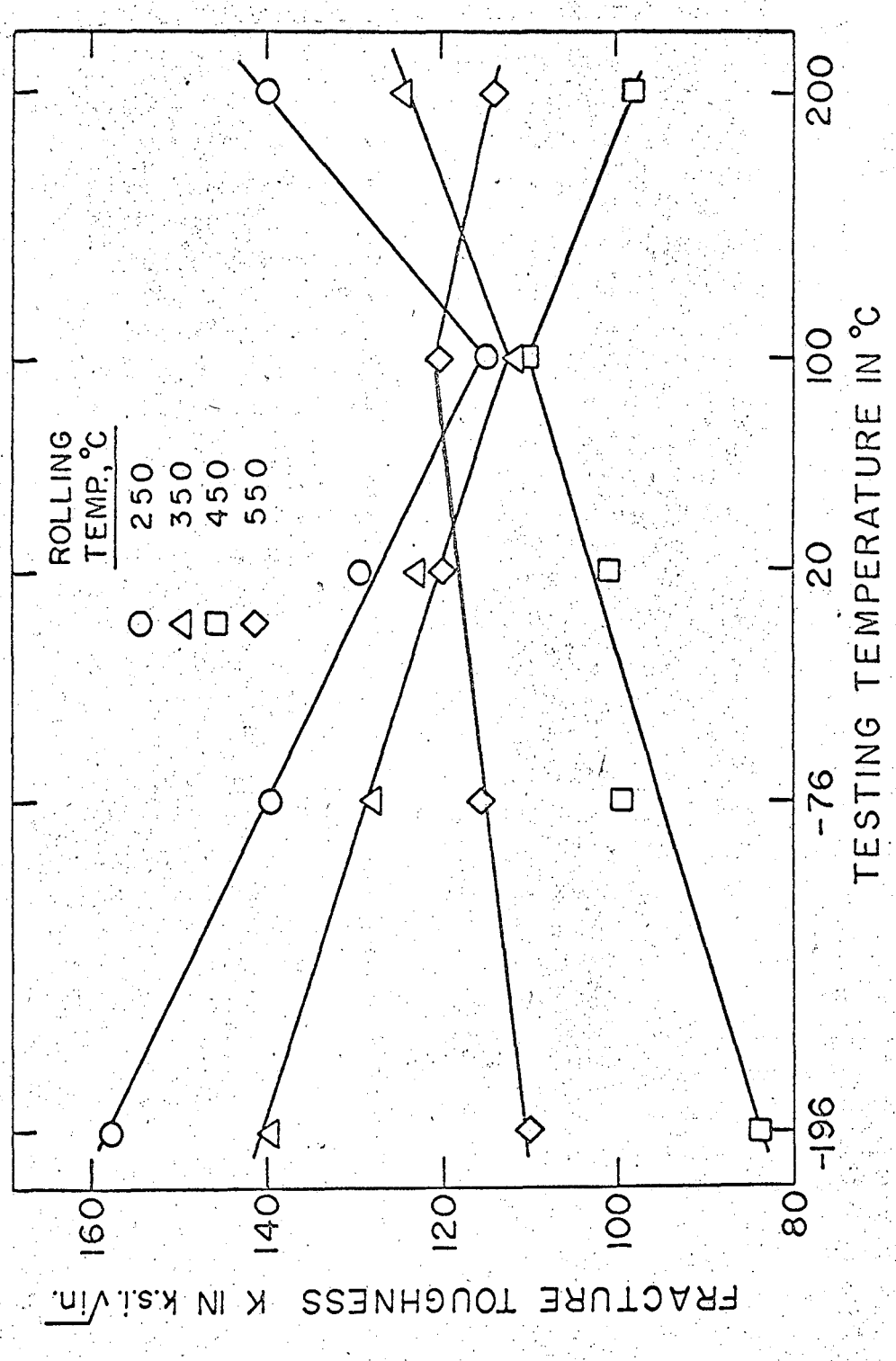
FRACTURE TOUGHNESS K IN k.s.i.√in.
160
140
120
100
80
TESTING TEMPERATURE IN °C
200
100
20
-76
-196
ROLLING TEMP., °C
250
350
450
550

Fig. 2

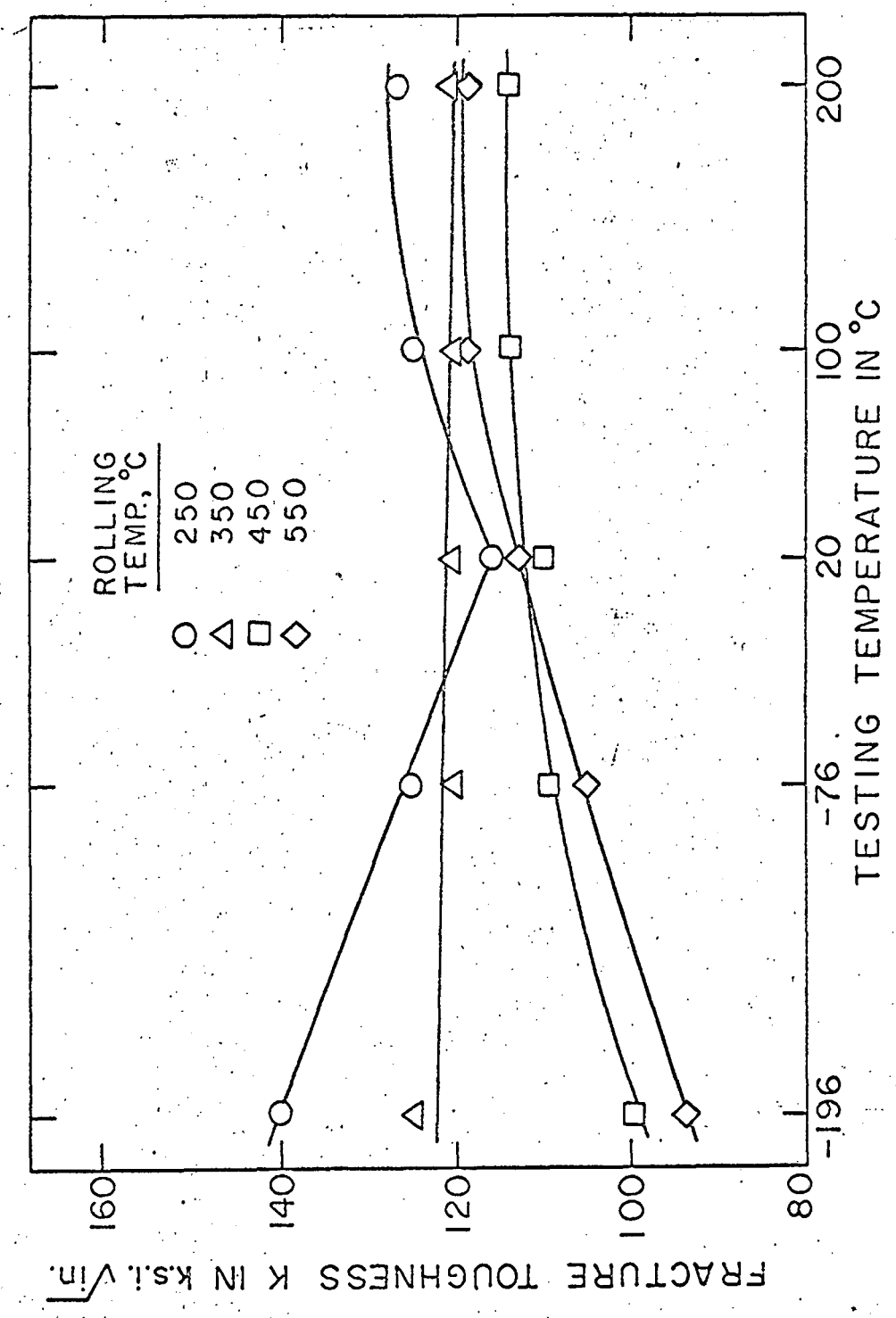
FRACTURE TOUGHNESS K IN k.s.i. √in.
160
140
120
100
80
-196
-76
20
100
200
TESTING TEMPERATURE IN °C
ROLLING TEMP., °C
250
350
450
550

Fig. 3

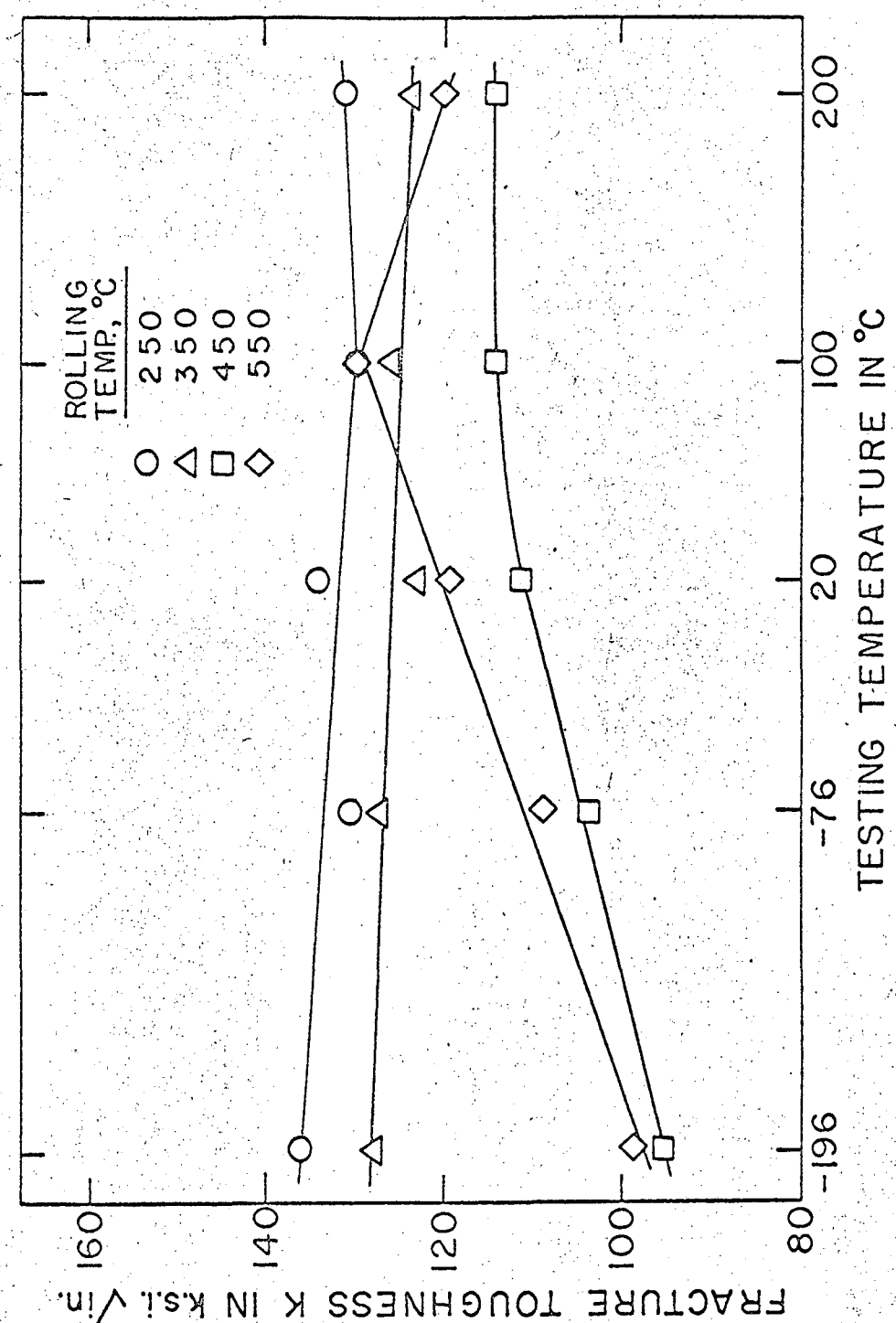
FRACTURE TOUGHNESS K IN k.s.i. √in.
160
140
120
100
80
-196
-76
20
100
200
TESTING TEMPERATURE IN °C
ROLLING TEMP., °C
250
350
450
550

Fig. 4

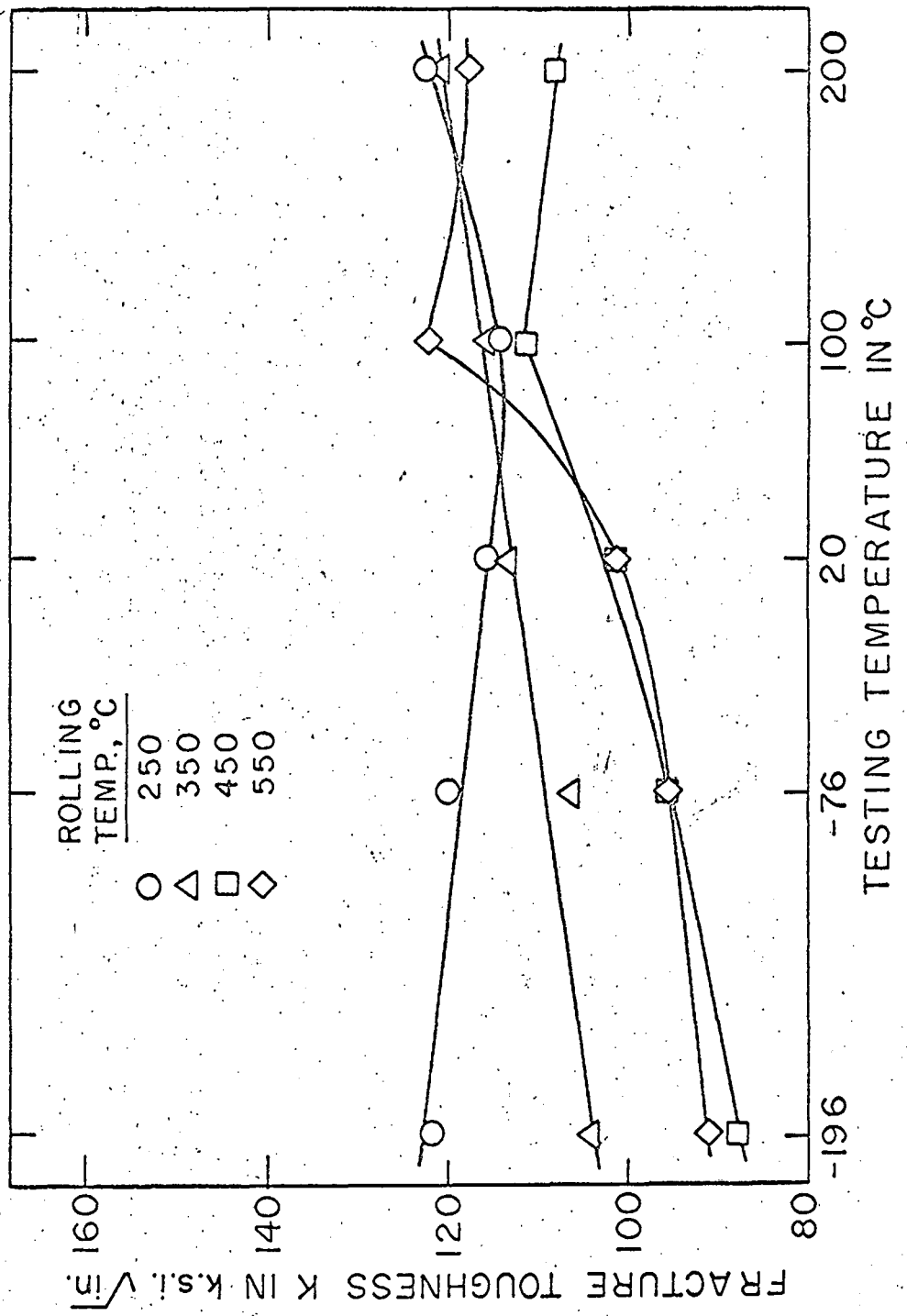
FRACTURE TOUGHNESS K IN k.s.i. √in.
160
140
120
100
80
TESTING TEMPERATURE IN °C
-196
-76
20
100
200
ROLLING TEMP., °C
250
350
450
550

Fig. 5

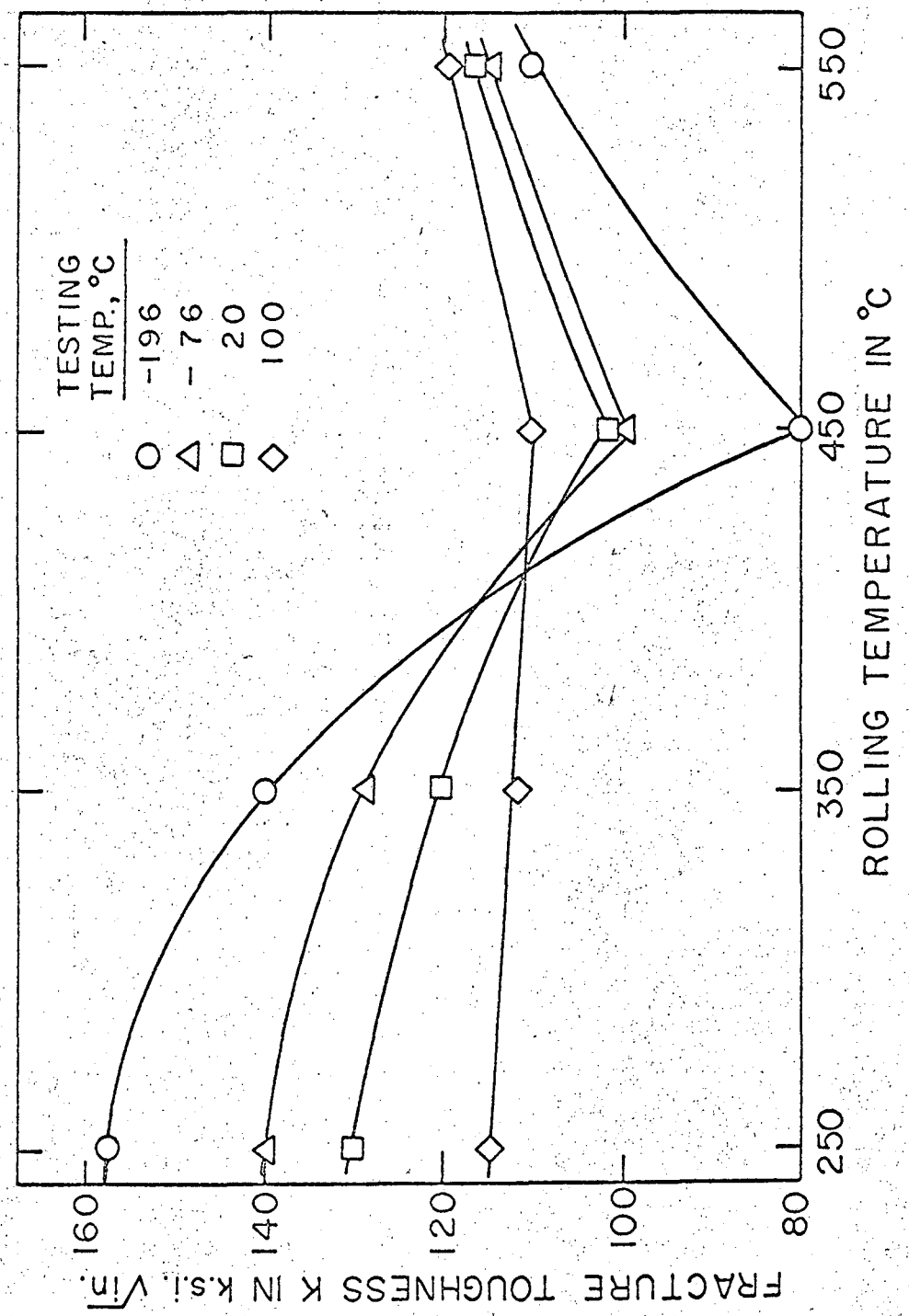
FRACTURE TOUGHNESS K IN k.s.i. √in.
160
140
120
100
80
250
350
450
550
ROLLING TEMPERATURE IN °C
TESTING TEMP., °C
-196
- 76
20
100

Fig. 6

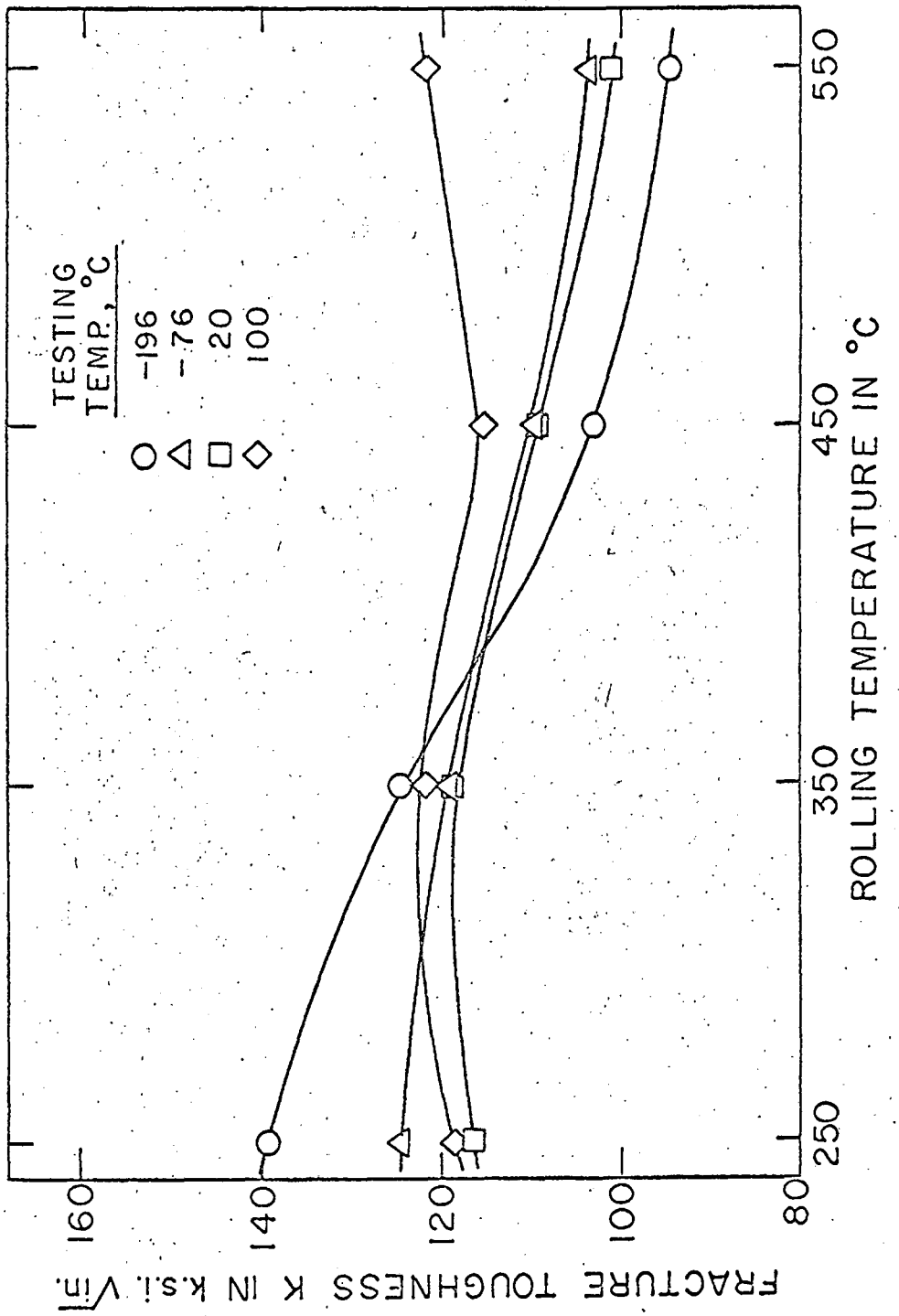
FRACTURE TOUGHNESS K IN k.s.i. √in.
160
140
120
100
80
250
350
450
550
ROLLING TEMPERATURE IN °C
TESTING TEMP., °C
-196
-76
20
100

Fig. 7

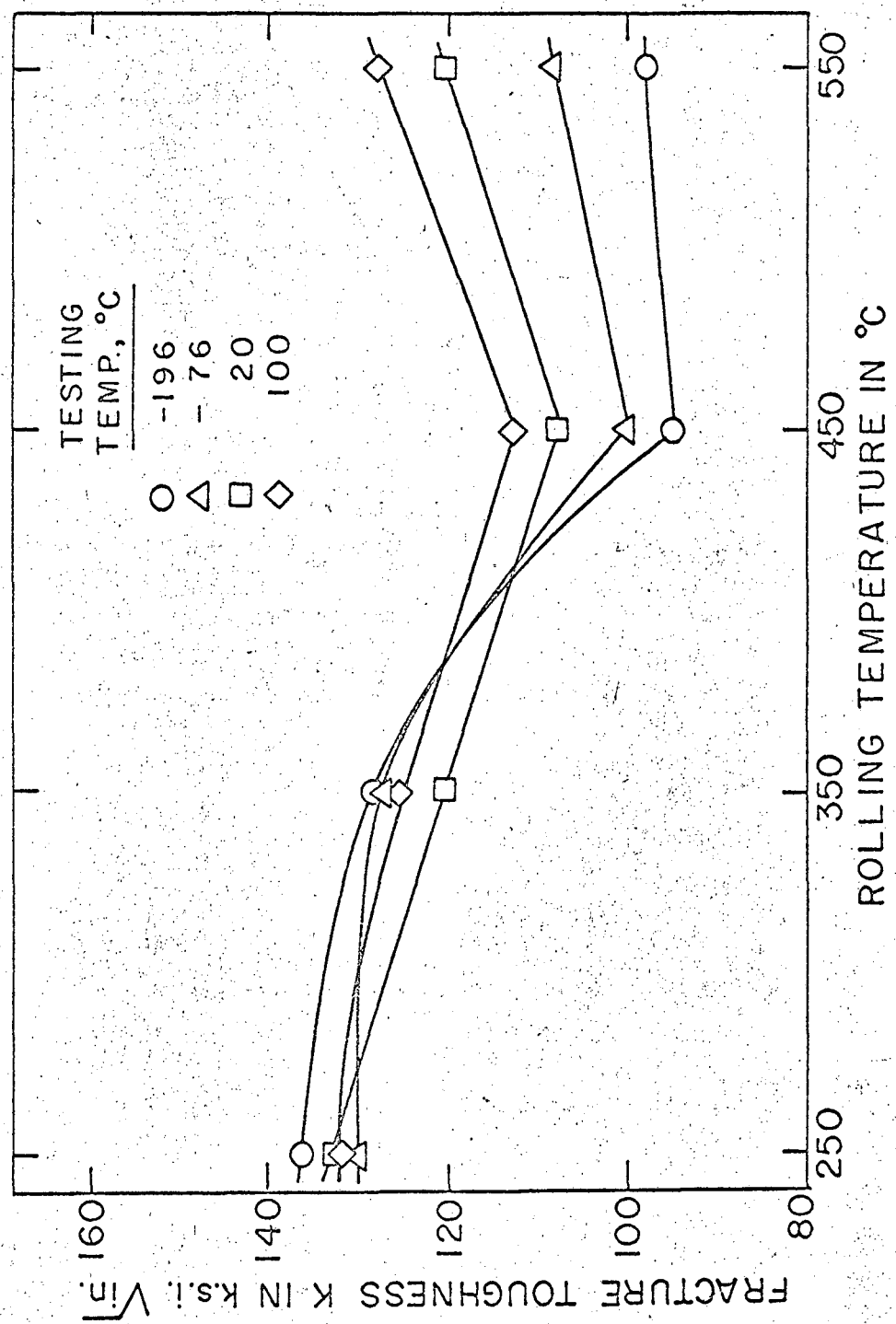
FRACTURE TOUGHNESS K IN k.s.i. √in.
160
140
120
100
80
250
350
450
550
ROLLING TEMPERATURE IN °C
TESTING TEMP., °C
-196
- 76
20
100

Fig. 8

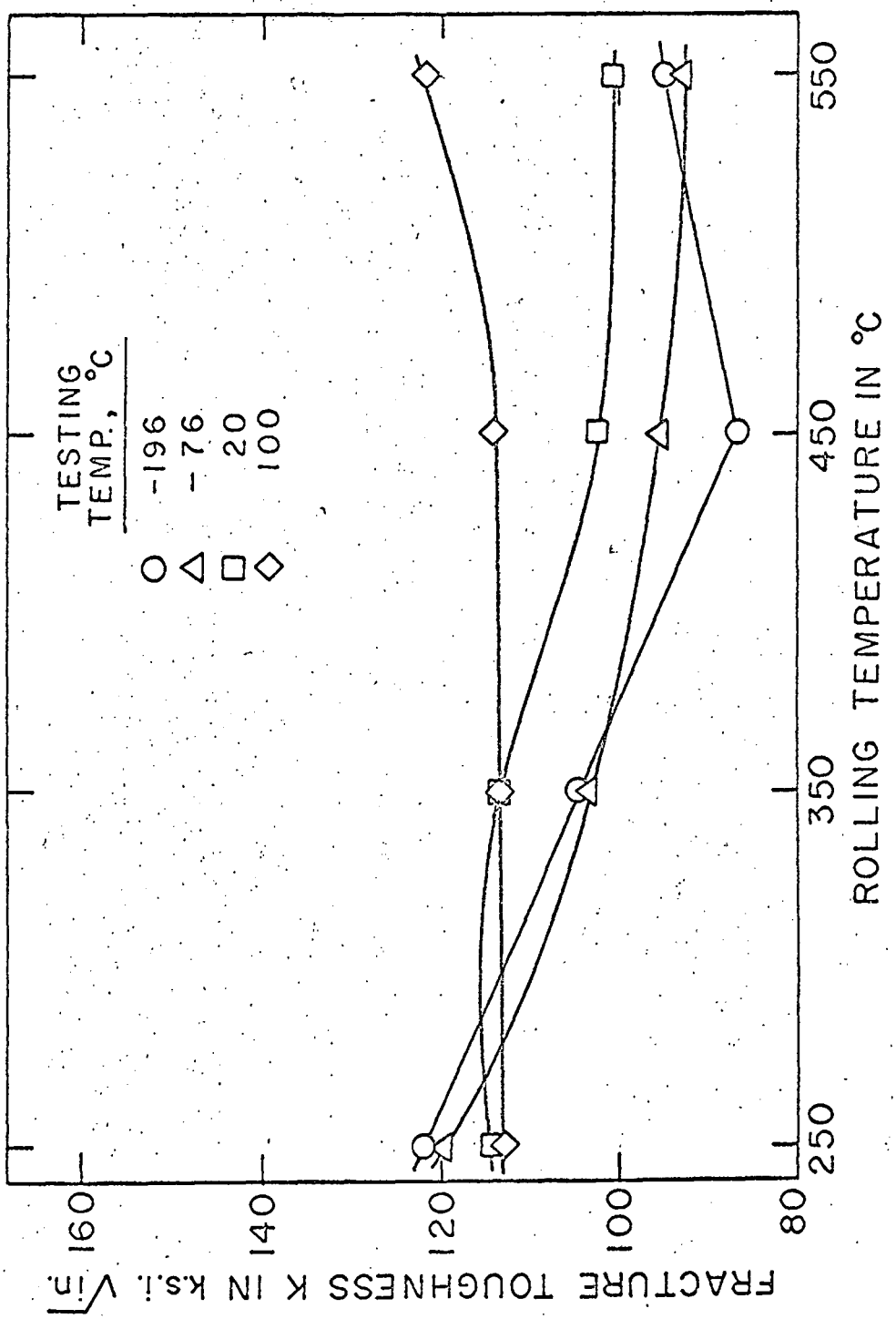
FRACTURE TOUGHNESS K IN k.s.i. √in.
160
140
120
100
80
250
350
450
550
ROLLING TEMPERATURE IN °C
TESTING TEMP., °C
-196
-76
20
100

Fig. 9

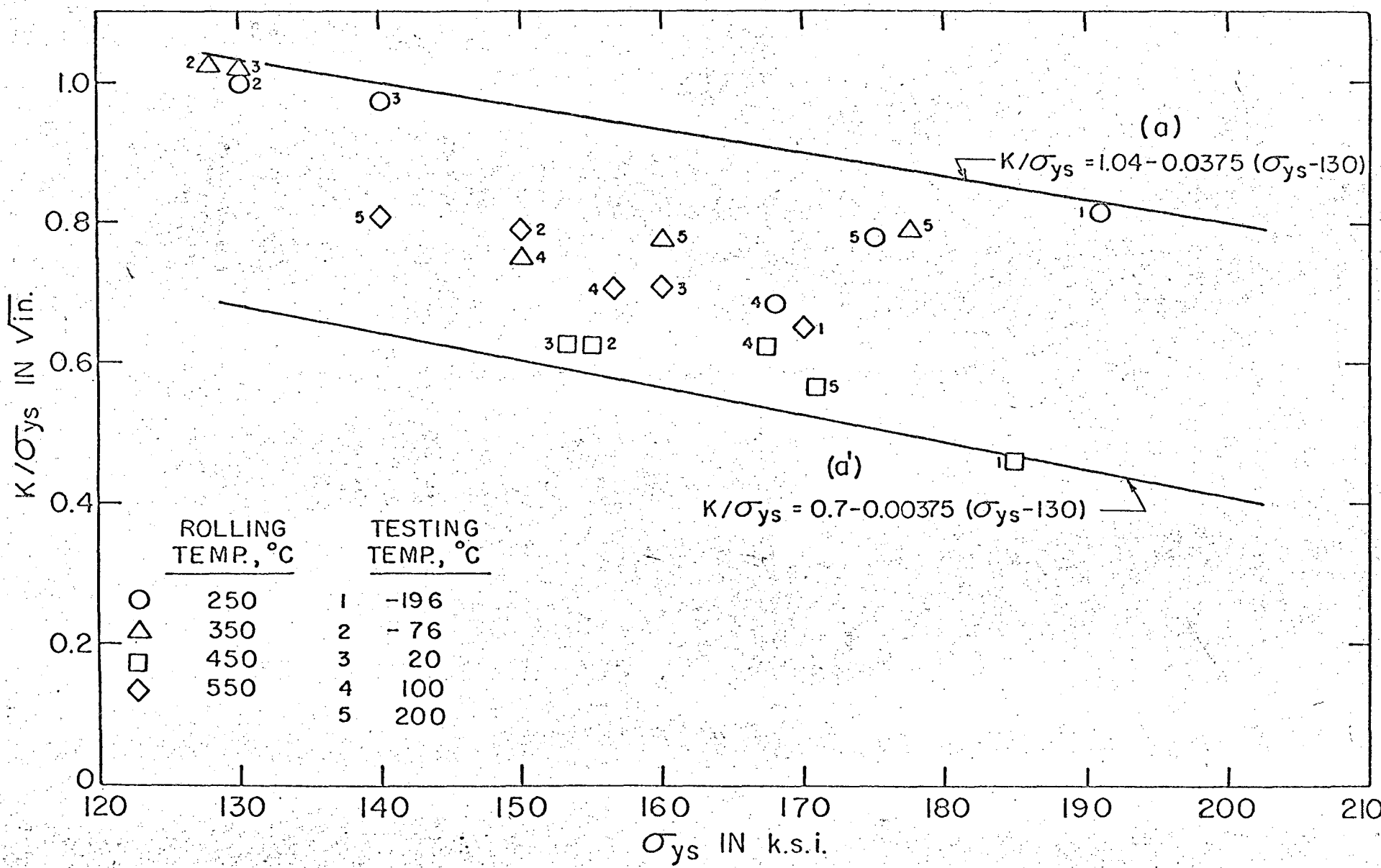
(a)
$K/\sigma_{ys} = 1.04 - 0.0375\ (\sigma_{ys} - 130)$
(a')
$K/\sigma_{ys} = 0.7 - 0.00375\ (\sigma_{ys} - 130)$
ROLLING TEMP., °C
250
350
450
550
TESTING TEMP., °C
1 -196
2 -76
3 20
4 100
5 200
K/σ_{ys} IN $\sqrt{in.}$
σ_{ys} IN k.s.i.
0
0.2
0.4
0.6
0.8
1.0
120
130
140
150
160
170
180
190
200
210

Fig. 10

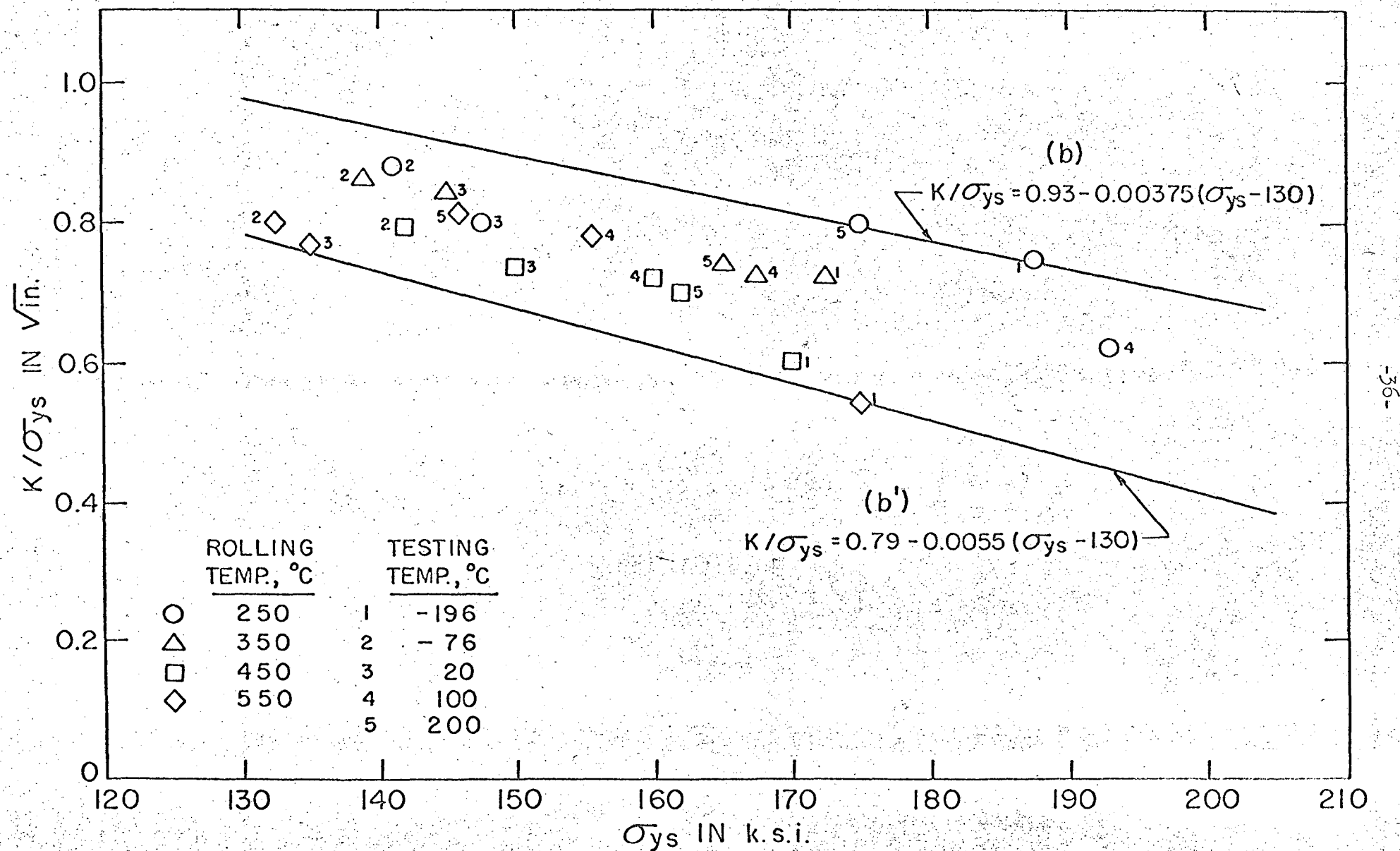
(b)
$K/\sigma_{ys} = 0.93 - 0.00375(\sigma_{ys} - 130)$
(b')
$K/\sigma_{ys} = 0.79 - 0.0055(\sigma_{ys} - 130)$
ROLLING TEMP., °C
250
350
450
550
TESTING TEMP., °C
1 -196
2 -76
3 20
4 100
5 200
K/σ_{ys} IN $\sqrt{in.}$
σ_{ys} IN k.s.i.
1.0
0.8
0.6
0.4
0.2
0
120
130
140
150
160
170
180
190
200
210

Fig. 11

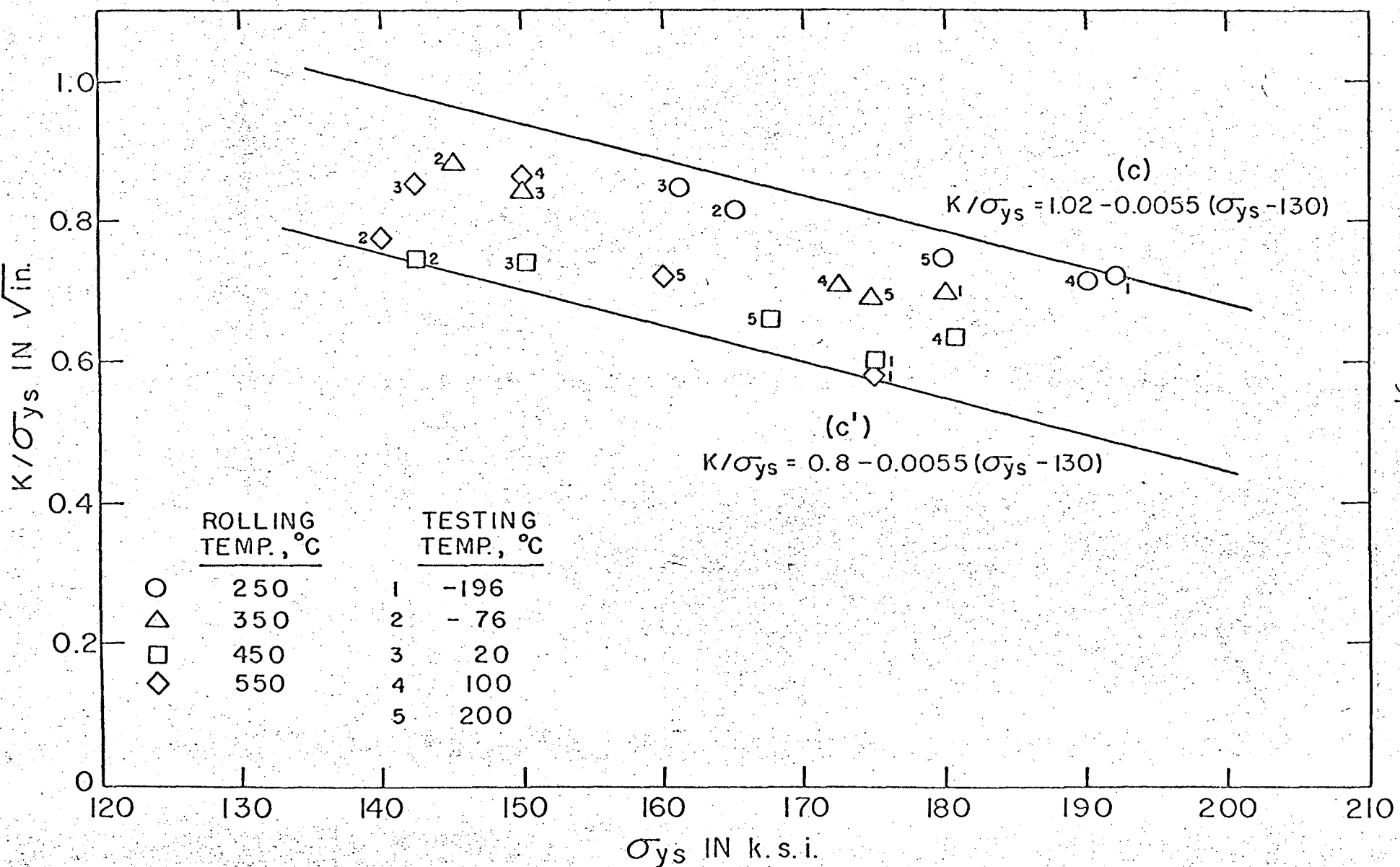
(c)
$K/\sigma_{ys} = 1.02 - 0.0055(\sigma_{ys} - 130)$
(c')
$K/\sigma_{ys} = 0.8 - 0.0055(\sigma_{ys} - 130)$
ROLLING TEMP., °C
250
350
450
550
TESTING TEMP., °C
1 -196
2 - 76
3 20
4 100
5 200
K/σ_{ys} IN $\sqrt{in.}$
σ_{ys} IN k.s.i.
0
0.2
0.4
0.6
0.8
1.0
120
130
140
150
160
170
180
190
200
210

Fig. 12

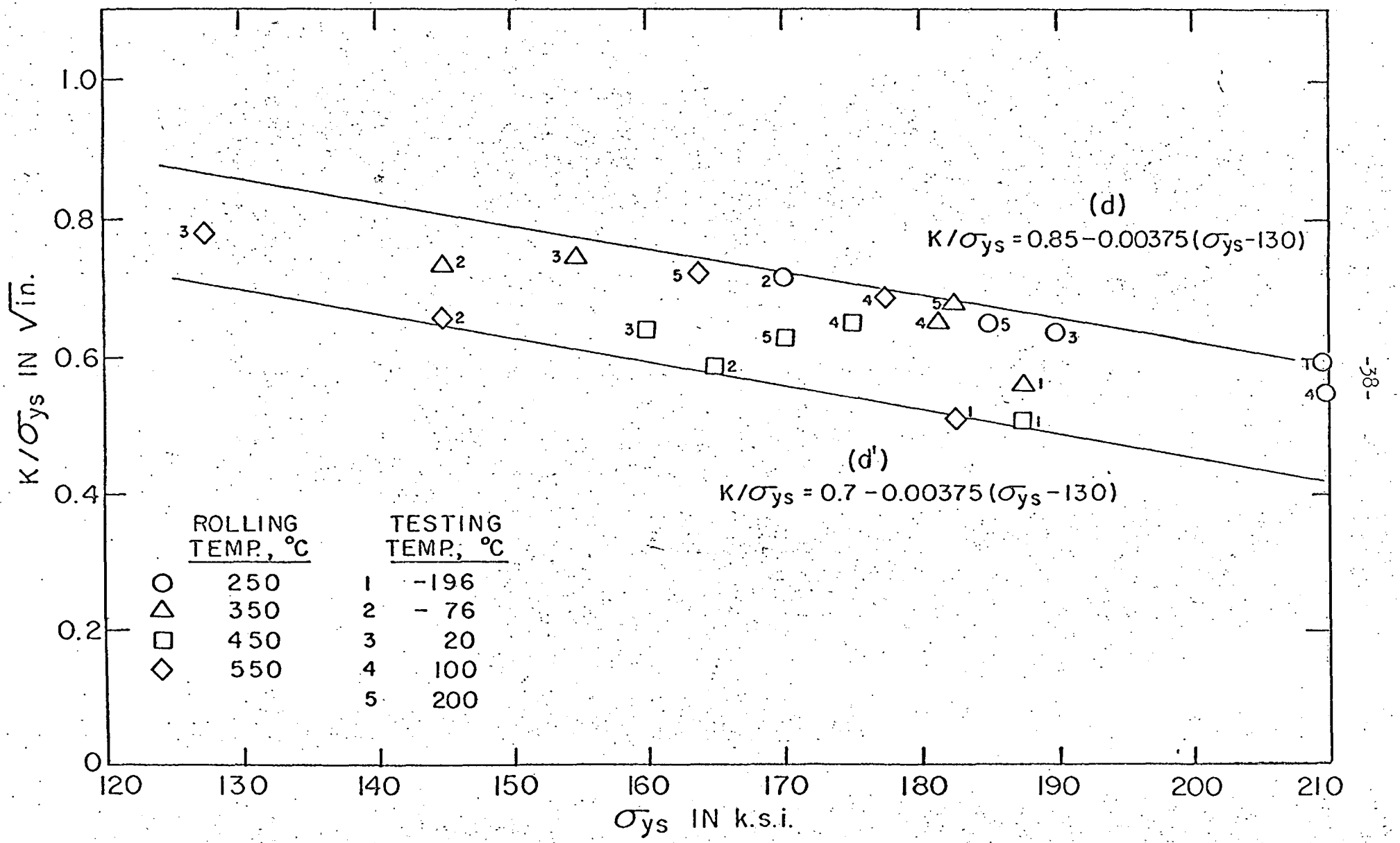
1.0
0.8
0.6
0.4
0.2
0
120
130
140
150
160
170
180
190
200
210
K/σ_{ys} IN $\sqrt{in.}$
σ_{ys} IN k.s.i.
(d)
$K/\sigma_{ys} = 0.85 - 0.00375(\sigma_{ys} - 130)$
(d')
$K/\sigma_{ys} = 0.7 - 0.00375(\sigma_{ys} - 130)$
ROLLING TEMP., °C
250
350
450
550
TESTING TEMP., °C
1 -196
2 - 76
3 20
4 100
5 200

Fig. 13

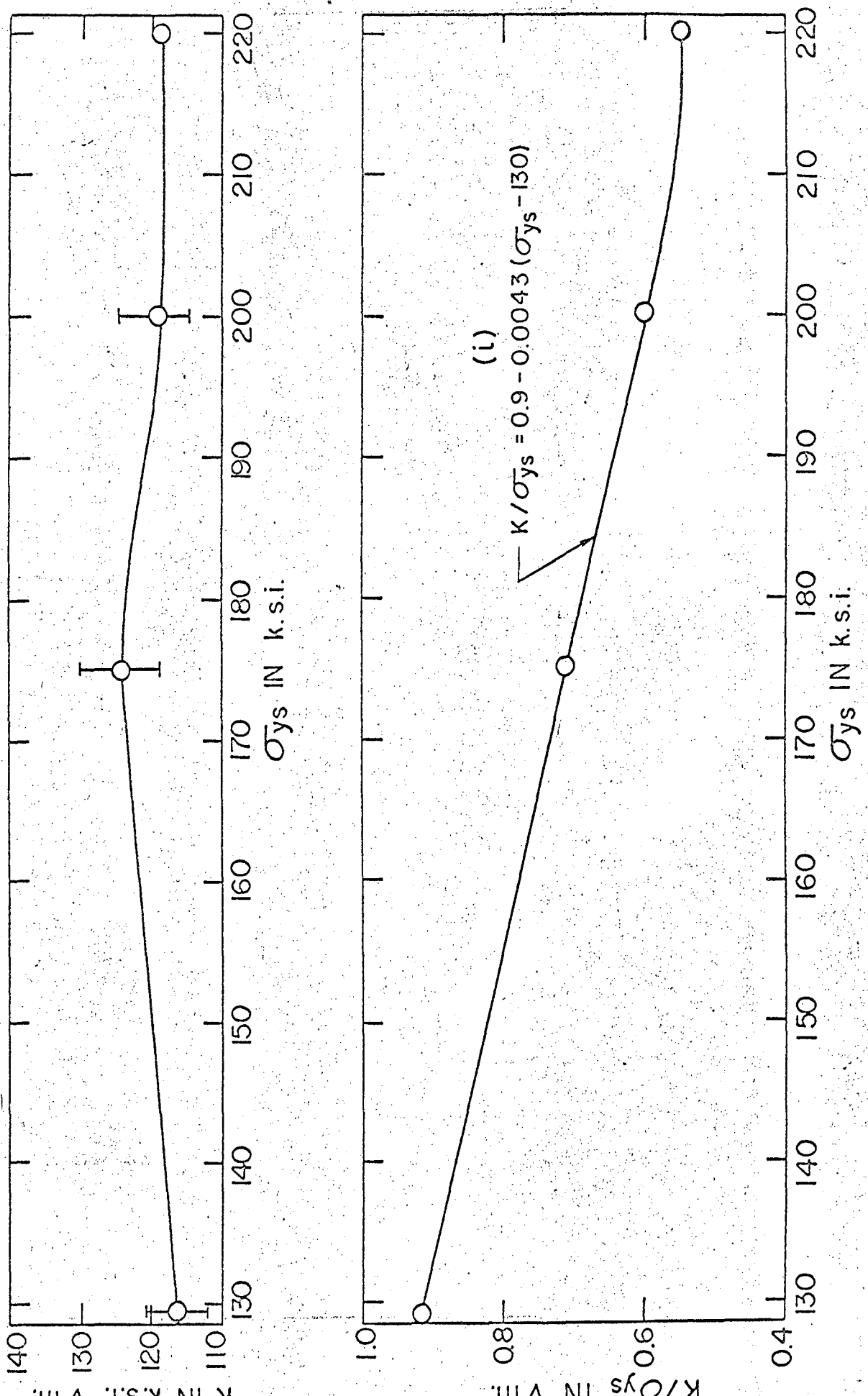
K IN k.s.i. √in.
140
130
120
110
130
140
150
160
170
180
190
200
210
220
σys IN k.s.i.
K/σys IN √in.
1.0
0.8
0.6
0.4
(i)
K/σys = 0.9 - 0.0043 (σys - 130)

Fig. 14

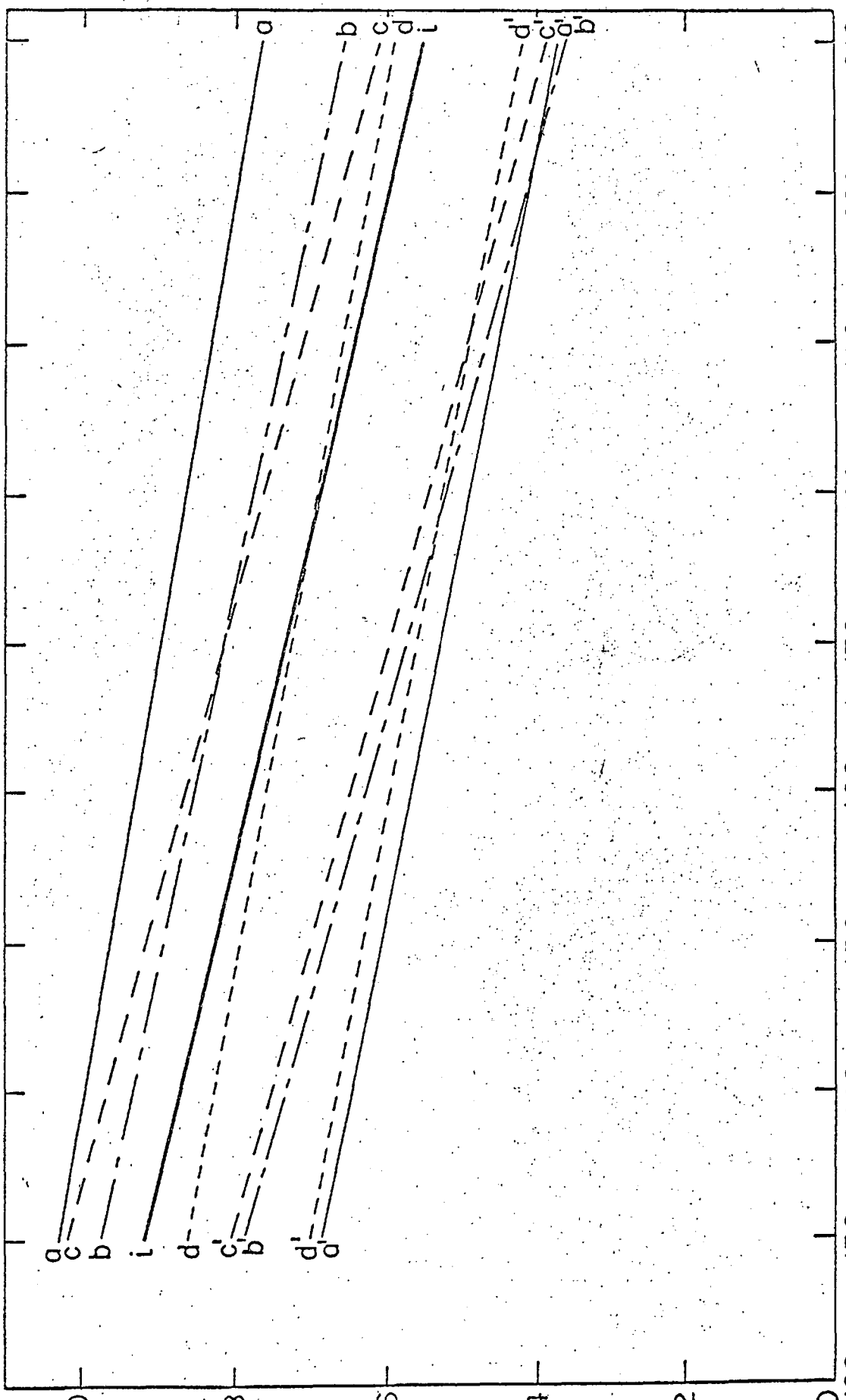
a
b
c
d
i
c'
b'
d'
a'
1.0
0.8
0.6
0.4
0.2
0
120
130
140
150
160
170
180
190
200
210
K/σ_{ys} IN $\sqrt{in.}$
σ_{ys} IN k.s.i.

Fig. 15

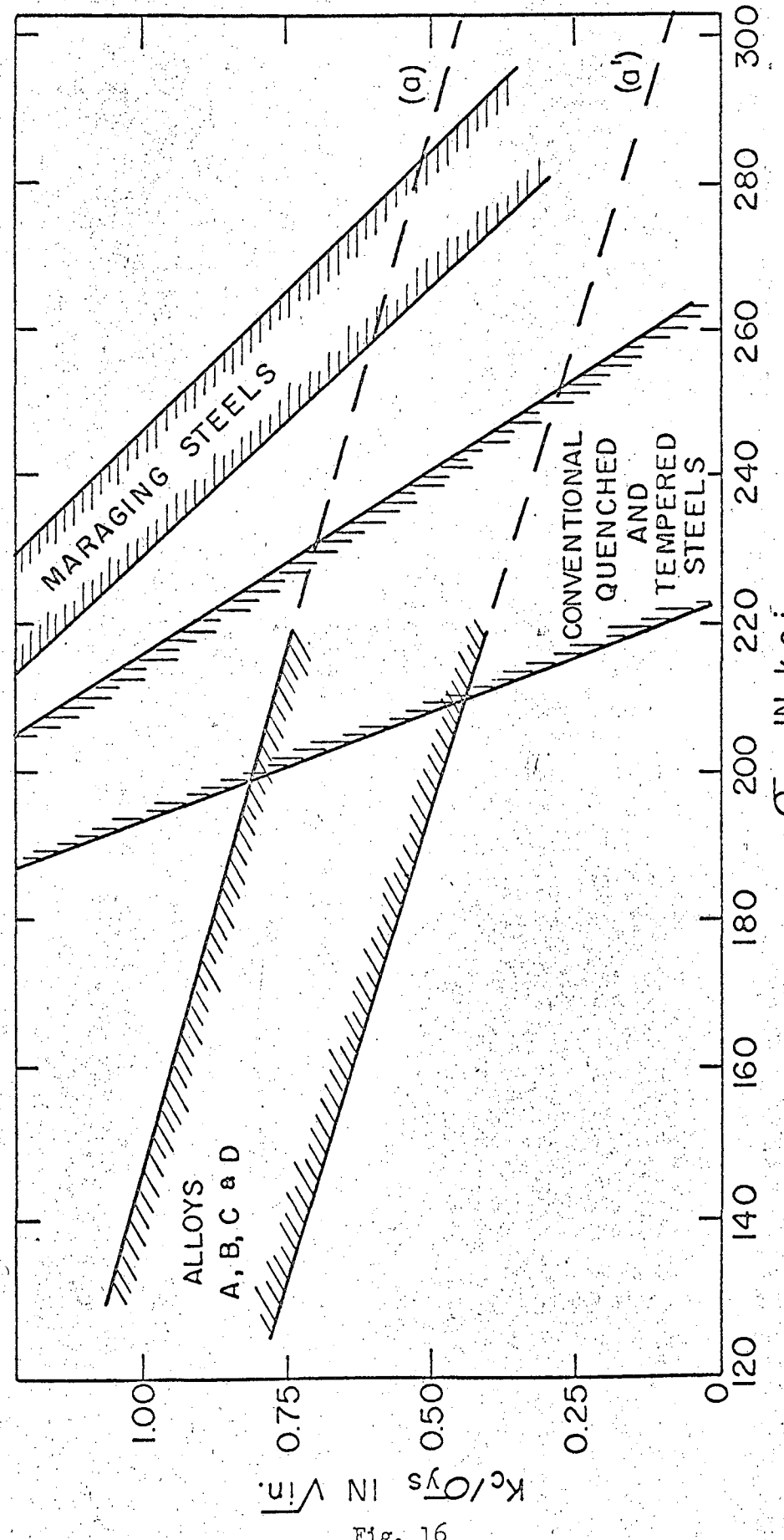
MARAGING STEELS
CONVENTIONAL QUENCHED AND TEMPERED STEELS
ALLOYS A, B, C & D
(a)
(a')
K_c/σ_{ys} IN $\sqrt{in.}$
σ_{ys} IN k.s.i.
1.00
0.75
0.50
0.25
0
120
140
160
180
200
220
240
260
280
300

Fig. 16

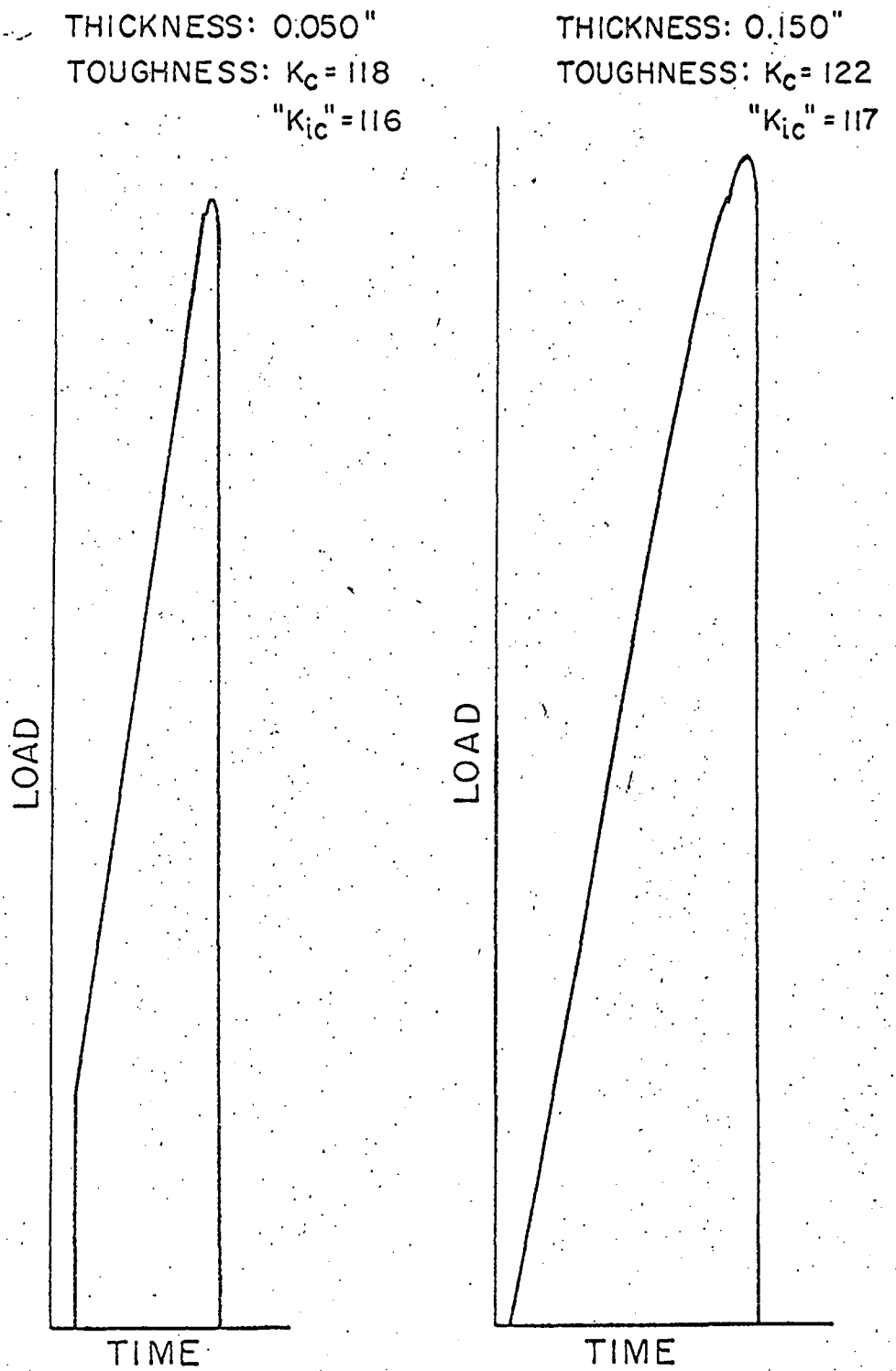
THICKNESS: 0.050"
TOUGHNESS: K_c = 118
"K_{ic}" = 116
LOAD
TIME
THICKNESS: 0.150"
TOUGHNESS: K_c = 122
"K_{ic}" = 117
LOAD
TIME

Fig. 17

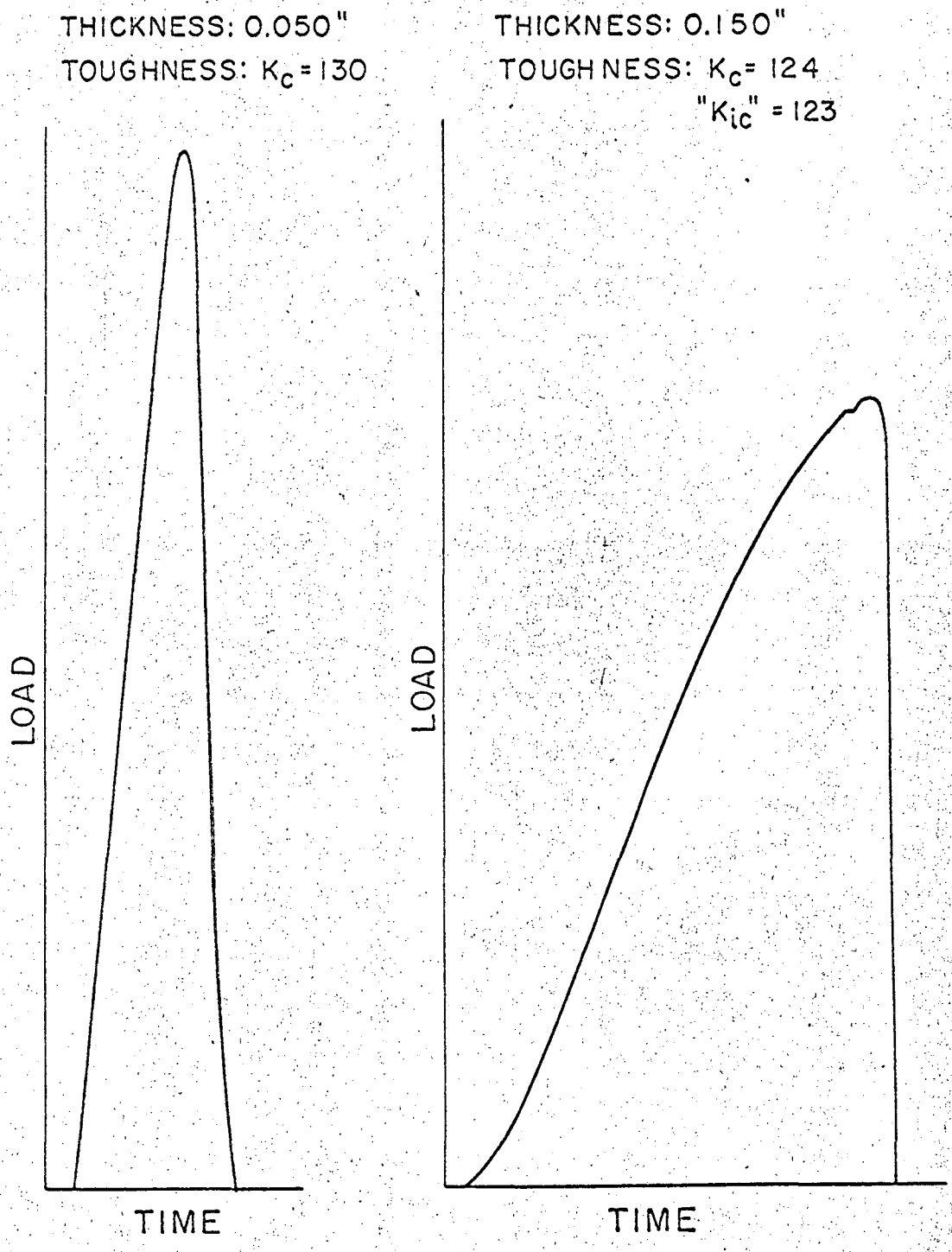
THICKNESS: 0.050"
TOUGHNESS: K_c = 130
LOAD
TIME
THICKNESS: 0.150"
TOUGHNESS: K_c = 124
"K_{ic}" = 123
LOAD
TIME

Fig. 18

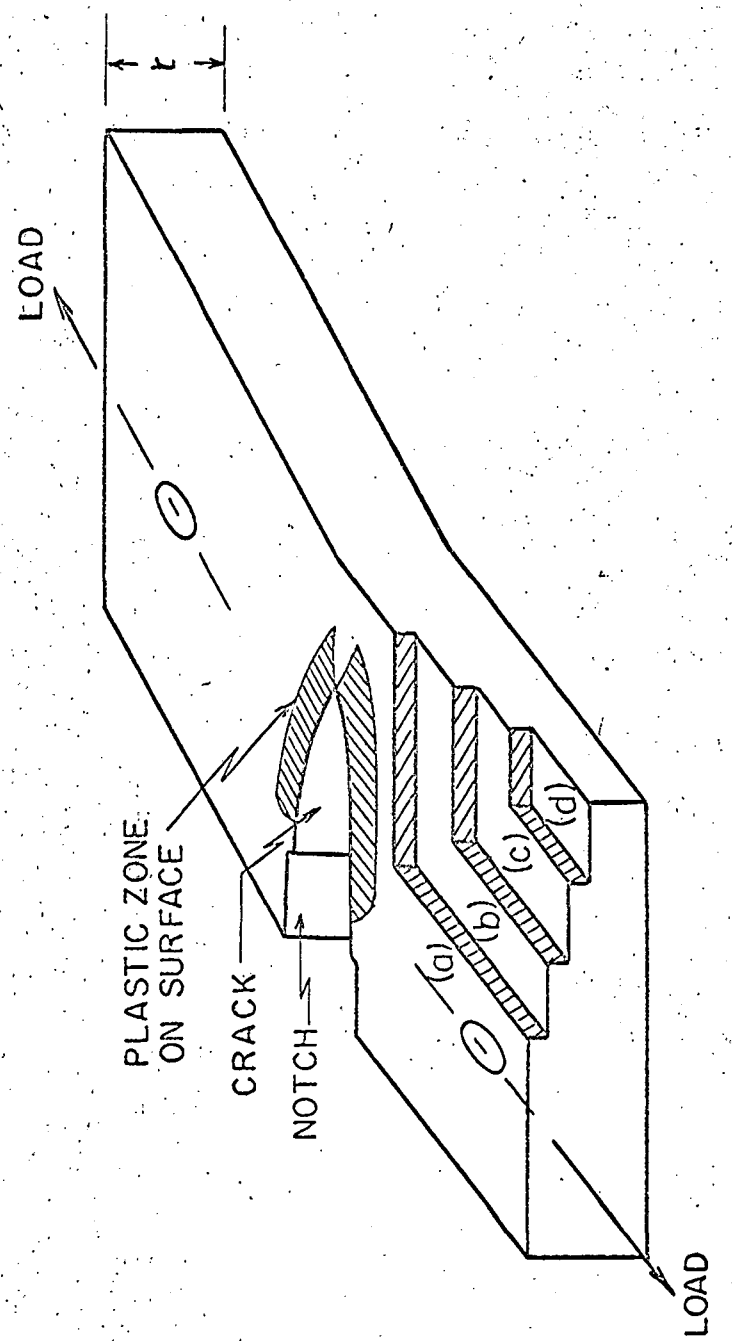

Fig. 19

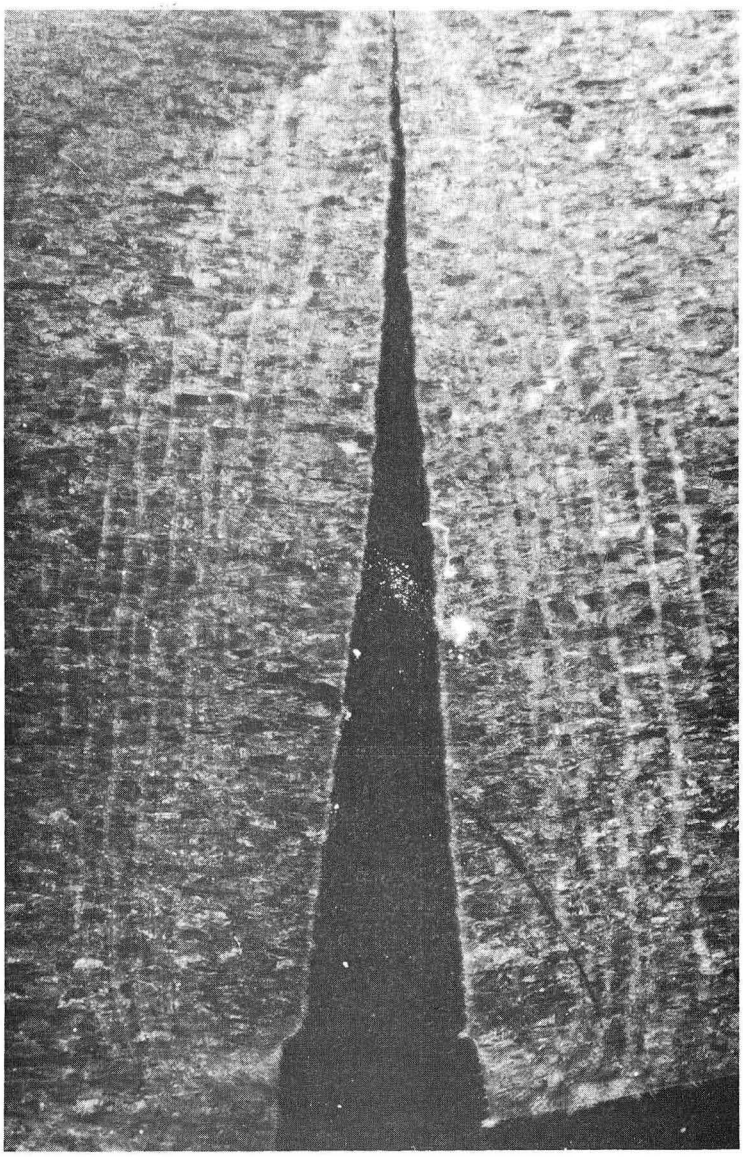

XBB 679-5725

Fig. 20

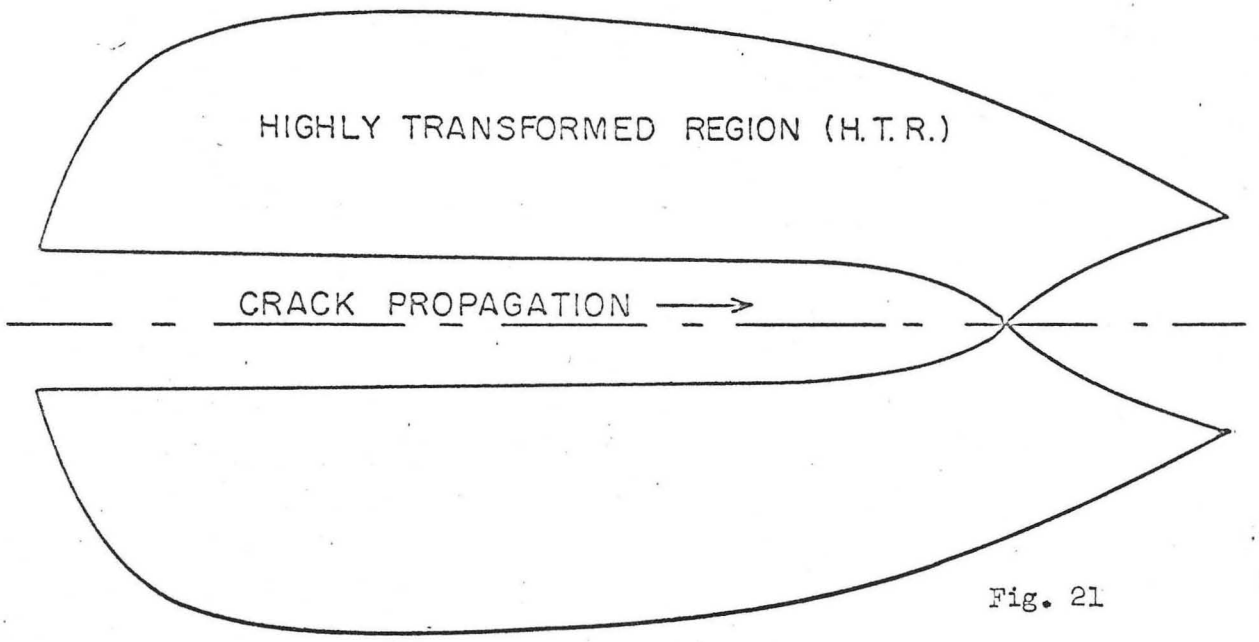

Fig. 21

SECTION (a)
DEPTH: SURFACE

Scale: 1 cm for 1 mm.

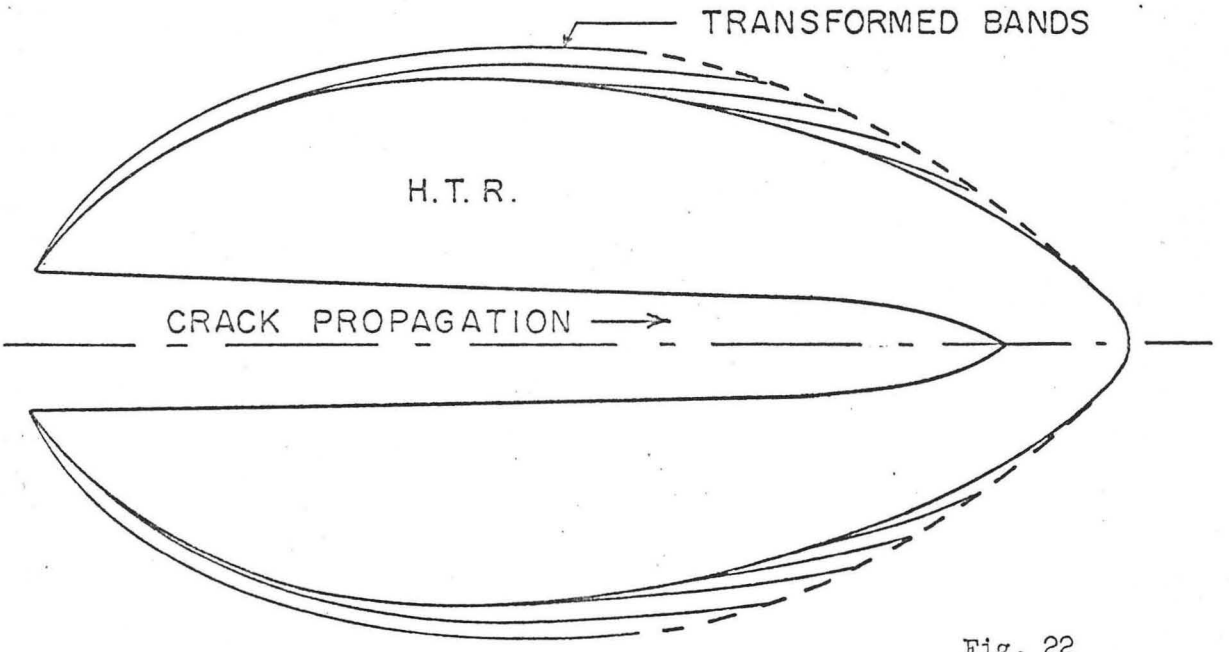

Fig. 22

SECTION (b)
DEPTH: 1/6 t

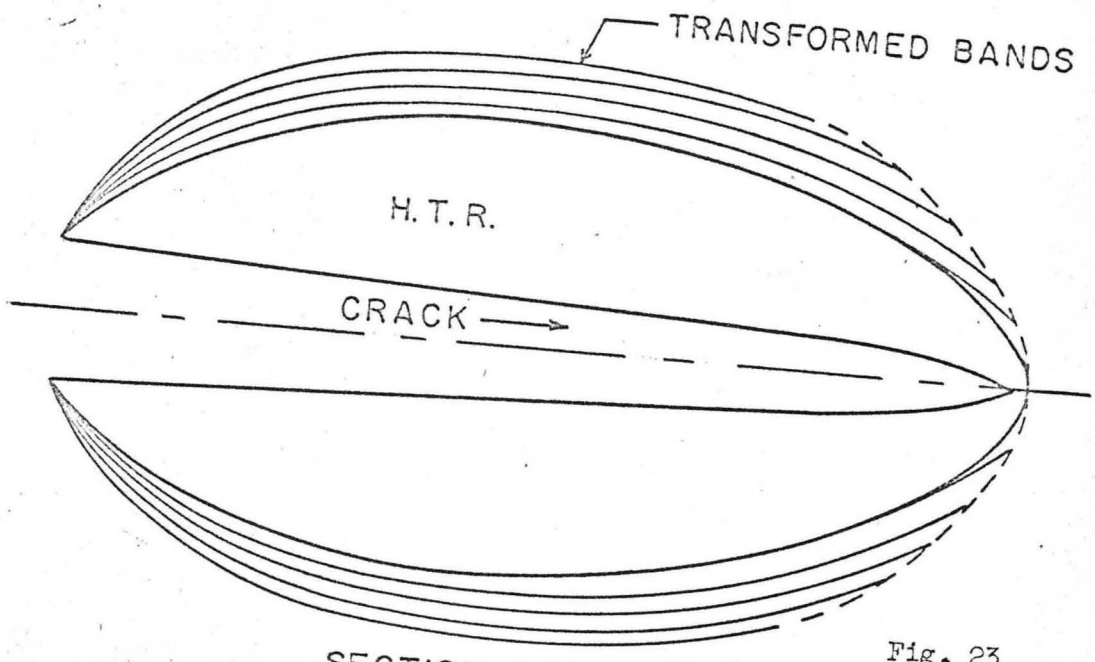

SECTION (c)
DEPTH: 1/3 t

Fig. 23

Sacle: 1 cm for 1 mm.

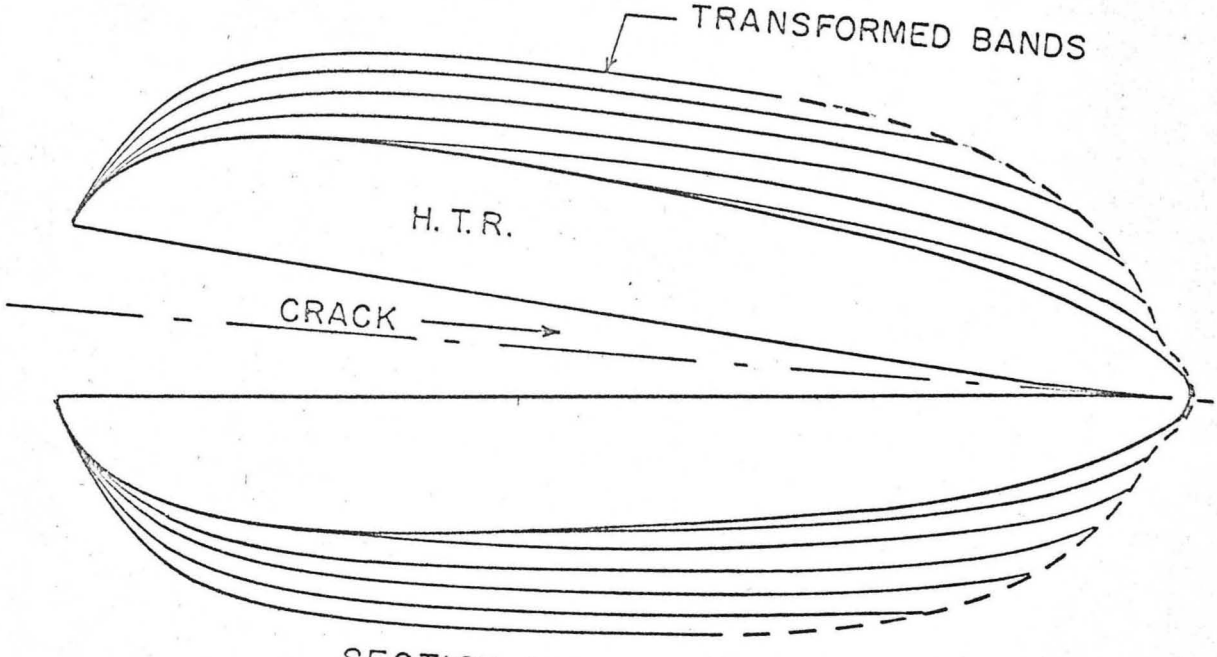

SECTION (d)
DEPTH: 1/2 t

Fig. 24

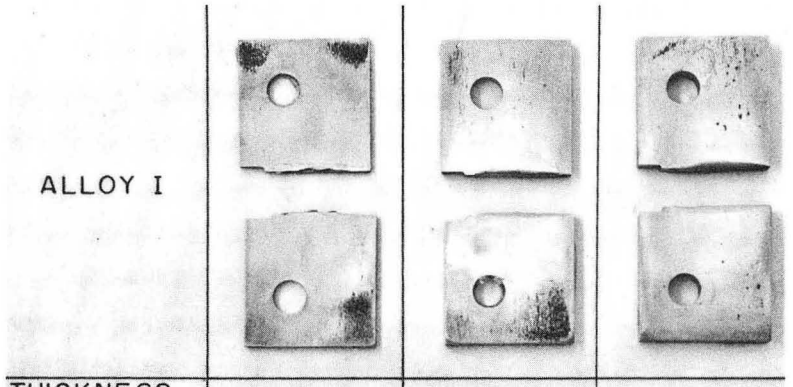

THICKNESS IN INCHES	0.050	0.100	0.150
TOUGHNESS IN k.s.i. $\sqrt{in.}$	108	98	94
Y.S. IN k.s.i.	133	145	148
U.T.S. IN k.s.i.	230	237	232
ELONGATION IN %	12	16	18

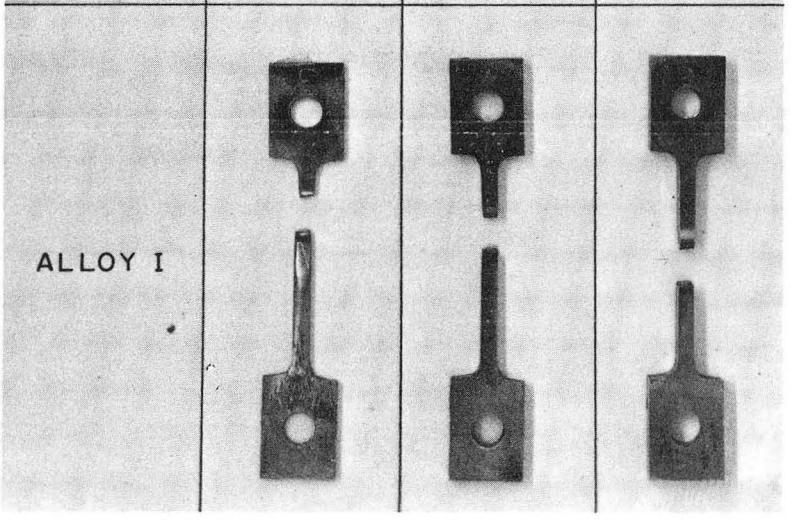

XBB 679-5726

Fig. 25

ALLOY H					
THICKNESS IN INCHES	0.050	0.100	0.150	0.200	0.240
TOUGHNESS IN k.s.i. $\sqrt{in.}$	150	150	148	147	141
Y.S. IN k.s.i	147	123	130	138	146
U.T.S. IN k.s.i.	204	158	192	198	206
ELONGATION IN %	18	22	25	25	29
ALLOY H					

XBB 679-5727

Fig. 26

DEFORMATION IN %	σ_{ys} IN k.s.i.	DUCTILITY IN %	U.T.S. IN k.s.i.	THICKNESS IN INCHES 0.050	0.100	0.150	0.200
20	127	42	163	K→ 119	114	112	120
40	175	36	190	K→ 130	120	124	122
60	200	26	195	K→ 118	125	122	
80	220	20	206	K→ 132			

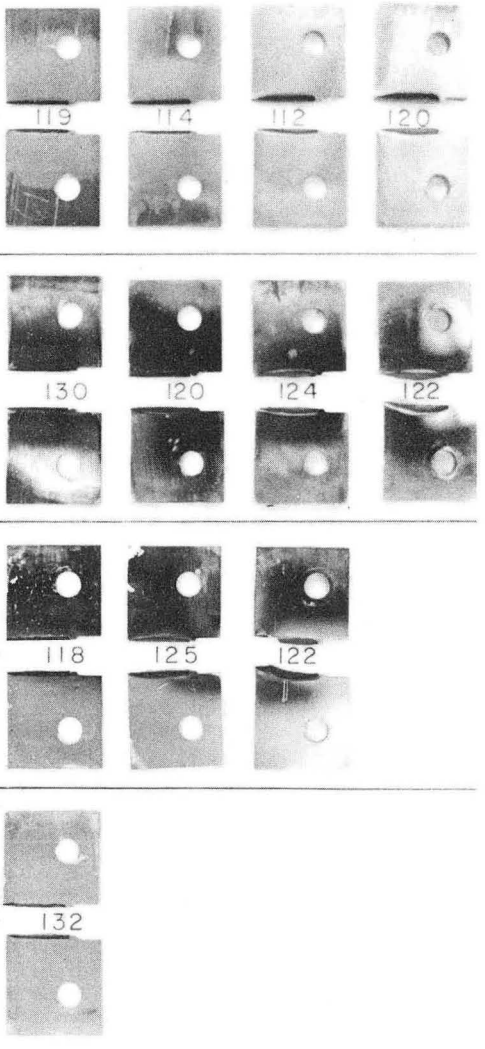

XBB 679-5728

Fig. 27